Metal Chalcogenide Modified Cobalt Oxide: Synthesis, Characterization and Photocatalytic Activity

By

Adeel Zia

A dissertation submitted in partial fulfillment of the requirements for the
Degree of Master of Science in Chemistry
Supervised by

Dr. Muhammad Fahad Ehsan

Department of Chemistry
School of Natural Sciences
National University of Sciences & Technology
Islamabad, Pakistan
2017

FORM TH-4

National University of Sciences & Technology

MS THESIS WORK

We hereby recommend that the dissertation prepared under our supervision by: ADEEL ZIA, Regn No. NUST201463669MSNS78214F Titled: Metal Chalcogenide Modified Cobalt Oxide: Synthesis, Characterization and Photocatalytic Activity be accepted in partial fulfillment of the requirements for the award of **MS** degree.

Examination Committee Members

1. Name: Dr. Muhammad Arfan Signature:

2. Name: Dr. Azhar Mahmood Signature:

External Examiner: Dr. Muhammad Naeem Ashiq Signature:

Co-Supervisor: Prof. Habib Nasir Signature:

Supervisor's Name: Dr. M. Fahad Ehsan Signature:

Head of Department

31-10-2017
Date

COUNTERSINGED

Date: 31/10/17

Dean/Principal

THESIS ACCEPTANCE CERTIFICATE

Certified that final copy of MS thesis written by **Mr. Adeel Zia**, (Registration No. **NUST201463669MSNS78214F**), of **School of Natural Sciences** has been vetted by undersigned, found complete in all respects as per NUST statutes/regulations, is free of plagiarism, errors, and mistakes and is accepted as partial fulfillment for award of MS/M.Phil degree. It is further certified that necessary amendments as pointed out by GEC members and external examiner of the scholar have also been incorporated in the said thesis.

Signature: ____________________
Name of Supervisor: Dr. M. Fahad Ehsan
Date: ____________________

Signature (HoD): ____________________
Date: 31-10-2017

Signature (Dean/Principal): ____________________
Date: 31-10-17

Acknowledgements

I am grateful to the Creator ***Almighty Allah*** *to have guided me throughout this work and for every new thought which He setup in my mind to enhance it. Every path He paved throughout this span, anyone who helped me for my thesis, whether my parents or any other individual was just because of His will, so to be sure none be worthy of praise but Him.*

I am generously thankful to my ***Parents*** *who raised me when I was not even capable of strolling and kept on supporting me.*

I would also like to appreciate my supervisor ***Dr. Muhammad Fahad Ehsan*** *for all the guideline and help he has provided during my research work and for his marvelous support and cooperation. Without all this, I would be unable to achieve my goal. I would also like to thank all faculty members of Chemistry Department at SNS for teaching me various taught courses that helped me a lot during my research phase.*

I would also extend my gratitude to my co-supervisor and HoD Chemistry, ***Prof. Dr. Habib Nasir****, my GEC members including* ***Dr. Muhammad Arfan*** *and* ***Dr. Azhar Mahmood Malik*** *for being on my thesis guidance and examination committee. I would also like to thank Principal SNS* ***Prof. Azad Akhter Siddiqui*** *for providing us all the required facilities to carry out research smoothly. Finally, I would like to acknowledge my lab fellows including* ***Memoona Qammar, Saba Bashir, Rabia Khan*** *and* ***Samia Qudoos*** *who have rendered valuable assistance, courage and motivations for my study.*

Adeel Zia

Dedicated to my beloved Parents Mr. & Mrs. Muhammad Zia Ullah

Abstract

Due to increasing energy demands and environmental pollution, it is need of the hour to develop some eco-friendly technologies that can overcome these two major issues. Nanotechnology and photocatalysis provide best solution for the energy crisis and environmental pollution. Here, in this work, we report various metal chalcogenides modified cobalt oxide photocatalysts (Co_3O_4, CoTe, ZnSe, Co_3O_4/CoTe and Co_3O_4/ZnSe) for the photocatalytic degradation of Congo red, which is a major industrial waste and pollution causing agent. Synthesized photocatalysts are further characterized by various techniques including powder X-ray diffraction (XRD), scanning electron microscopy (SEM) coupled with energy dispersive X-ray spectroscopy (EDX) and UV-Visible diffused reflectance spectroscopy. These techniques have confirmed that nanoparticles and their nanocomposites have been synthesized successfully. Among different synthesized photocatalysts, it was expected that nanocomposites (Co_3O_4/ZnSe, Co_3O_4/CoTe) would show better photocatalytic activities as compared to their individual counter parts which might be ascribed to the reduced electron-hole recombination. In case of Co_3O_4/CoTe nanocomposite photocatalytic activity is high, which was about 96 % in 60 min for the degradation of Congo red. But the photocatalytic activity of pure Co_3O_4, CoTe is just 20 % and 15 %, respectively. The higher photocatalytic activity of Co_3O_4/CoTe is attributed to high charge separation, better bandgap alignment and presence of common cation. As far as the photocatalytic activity of Co_3O_4/ZnSe nanocomposite is concerned, unexpected results were obtained because bare ZnSe has shown better photocatalytic activity which was about 98 % in 60 min as compared to its nanocomposite which was near 94 % in 60 min for the photodegradation of Congo red dye. This might be attributed to the presence of mixed phase of ZnSe *i.e.* cubic and hexagonal, which makes ZnSe itself a heterostructure to facilitate charge separation.

Table of Contents

1 Chapter 1: Introduction and Literature Survey 1

1.1 Introduction 1

1.2 Recent Problems 1
  1.2.1 Environmental Pollution 1
  1.2.2 Energy Crisis 3

1.3 Solutions of the Problems 7
  1.3.1 Reduce Personal Consumption 7
  1.3.2 Recycling and Reforestation 7
  1.3.3 Use Clean and Renewable Resources of Energy 8
  1.3.4 Introduction of Eco-Friendly and Efficient Technologies 9

1.4 Nanotechnology 9
  1.4.1 Types of Nano Materials 9
  1.4.2 Synthesis of Nanomaterials 10
  1.4.3 Properties of Nanomaterials 14
  1.4.4 Applications of Nanomaterials 19

1.5 Characterization Techniques 23
  1.5.1 X-ray Powder Diffraction 23
  1.5.2 Scanning Electron Microscopy 25
  1.5.3 Energy Dispersive Spectroscopy 27
  1.5.4 UV-VIS Spectroscopy 29

1.6 Photocatalytic Activity 31

1.7 Scope of This Work 31

2 Chapter 2: Experimentation 33

Experimental Details 33

2.1 Hydrothermal Synthesis of Co_3O_4 Nanoparticles 33

2.2 Hydrothermal Synthesis of ZnSe Nanoparticles 34

2.3 Hydrothermal Synthesis of CoTe 35

2.4 Synthesis of Different Composites of Co_3O_4/ZnSe and Co_3O_4/CoTe 36

3 Chapter 3: Co_3O_4/CoTe Common- Cation Nanocomposite 38

3.1 Crystallographic Analysis 38

3.2 Morphological Analysis 39

3.3 Elemental Analysis 41

3.4 Optical Properties and Bandgap Estimation 45

3.5 Photocatalytic Activity of Co_3O_4/CoTe 48
3.6 Mechanism of Photocatalysis 49
4 Chapter 4: Co_3O_4/ZnSe Nanocomposite 51
4.1 Crystallographic Analysis 51
4.2 Morphological Analysis 52
4.3 Elemental Analysis 54
  4.3.1 Optical Studies and Bandgap Estimation 57
4.4 Photocatalytic Activity of Co_3O_4/ZnSe 58
4.5 Conclusion 59
5 Chapter 5: Conclusion and Future Prospects 60
5.1 Conclusion 60
5.2 Future Prospects 61
References 62

List of Figures

Figure 1.1. Fundamental factors of pollution... 2
Figure 1.2. Diseases caused by pollution... 3
Figure 1.3. Sources of Energy Production [Adapted from Ref. 11]............................ 4
Figure 1.4. Global energy consumption during 2006-2030 [Adapted from Ref. 8]...... 6
Figure 1.5. Top-down and bottom-up approach for synthesis of nanomaterials 11
Figure 1.6. Appearance of blue shift due to reduction in size in CdSe quantum dot.. 15
Figure 1.7. Mechanism of photocatalysis 16
Figure 1.8. Sensitization of photocatalyst.. 17
Figure 1.9. Heterostructure for photocatalysis 18
Figure 1.10. Cocatalyst assisted photocatalysis [Adapted from Ref. 58].................. 19
Figure 1.11.XRD Machine…………………………………………………...…24
Figure 1.12 Schematic Diagram of X-ray diffractometer…………………..……….25
Figure 1.13. Schematic diagram of SEM…………………………………………27
Figure 1.14 Emission of X-ray [Adapted from Ref. 94]…………………......…27
Figure 1.15. Schematic diagram of EDX……………………………….…………28
Figure 1.16. Energy of the orbitals and modes of possible transitions……………....30
Figure 1.17. Schematic diagram of UV-Vis spectrophotometer……………….…30
Figure 2.1. Autoclave and teflon tube…………………………………….…………33
Figure 2.2. General flow sheet diagram for the hydrothermal synthesis of nanoparticles…………………………………………………………………………36

Figure 2.3. Mortar and Pestle 36
Figure 3.1. XRD patterns of (a) Co_3O_4, (b) CoTe, (c) Co_3O_4/CoTe (3:1), (d) Co_3O_4/CoTe (1:1) and (e) Co_3O_4/CoTe (1:3) 39
Figure 3.2. SEM images of (a) Co_3O_4 and (b) CoTe.. 40
Figure 3.3. SEM Image of Co_3O_4/CoTe nanocomposites (a) A1, (b) A2 and (c) A3…………………………………………………………………………………40
Figure 3.4. EDX analysis of (a) Co_3O_4 and (b) CoTe……………………………41
Figure 3.5. EDX analysis of Co_3O_4/CoTe nanocomposites (a) A1, (b) A2 and (c) A3…………………………………………………………………………………43
Fifure 3.6. (a) UV-Vis spectrum and (b,c) Tauc plots of Co_3O_4 ……………………46
Figure 4.1. XRD pattern of (a) Co_3O_4, (b) ZnSe, (c) Co_3O_4/ZnSe (3:1), (d) Co_3O_4/ZnSe (1:1) and (e) Co_3O_4/ZnSe (1:3) 52
Figure 4.2. SEM images of ZnSe 52
Figure 4.3. SEM images of Co_3O_4/ZnSe nanocomposites (a) Z1, (b) Z2 and (c) Z3..53
Figure 4.4. EDX analysis of ZnSe…………………………………………………54
Figure 4.5. EDX analysis of composite (a) Z1, (b) Z2 and (c) Z3 …………………..55
Figure 4.6. (a) UV-Vis spectrum and (b) Tauc plot of ZnSe……………...………57
Figure 4.7. Bandgap alignment of Co_3O_4/ZnSe……………………………………...58
Figure 4.8. Dye degradation by (a) blank (b) Co_3O_4 (c) Co_3O_4/ZnSe (d) bare ZnSe photocatalysts……………………………………………………………………...59

Chapter 1: Introduction and Literature Survey

1.1 Introduction

We are living in the era of science and technology. From the last century, research in science and technology increased tremendously that resulted in rapid industrialization and revolutionized the life of mankind. We are enjoying much better facilities of transportation, communication and healthcare etc. as compared to our forefathers and these all are blessings of science and technology. But there are also some serious concerns about energy and environment that are related to this rapid growth of industrialization [1]. Due to excessive consumption of fossil fuels (petroleum, coal and gas), environment and ecosystem are being contaminated with hazardous materials and gases. Air, water and soil pollution is increasing. This pollution is a result of the boom in industrialization [2] and population growth which are affecting the health of both, flora and fauna of the earth.

1.2 Recent Problems

The modern world is facing many social, economical and ecological problems but climate changes [3], global warming, acid rain, ozone depletion, pollution, shortage of fuel and energy [4] are the most alarming issues that must be resolved.

1.2.1 Environmental Pollution

One of the most dangerous problems human beings are facing is environmental pollution [5] and it is increasing constantly. The environment encompasses all physical and biological components of the earth and environmental pollution is contamination of hazardous materials in these components. It results in the discomfort of these natural components and causes natural disasters and damage life on earth [6].

Nature has a capacity to restore itself by recycling and reabsorbing the hazardous substances but our rate of contamination (high-level production, consumption and throw out) is much higher as compared to the natural rate of reabsorbing and neutralizing the uncomfortable changes [2]. Our ways of production, consumption and recycling are dirty, inefficient and full of carelessness which is the cause of environmental pollution.

- **Fundamental Factors of Pollution**

Up to some extent, pollution is known to human beings from prehistoric time especially when fire had been invented. But due to rapid industrialization since last century, pollution becomes a serious issue because it has devastating effects on our environment. From last 200 years, several fundamental factors arise that are the basic causes of water, air and land pollution.

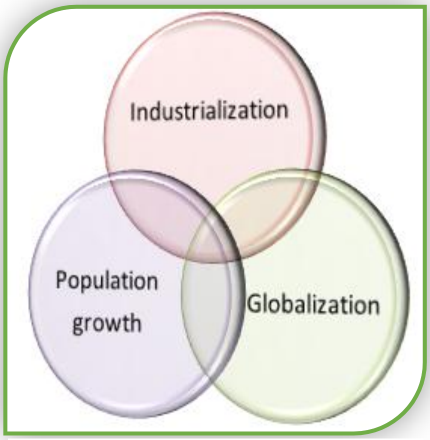

Figure 1.1. Fundamental factors of pollution

- **Industrialization**

It is the first fundamental cause of pollution. Fossil fuel (coal, gas & oil) burning [5] in industries and other industrial wastes are the main sources of pollution because smoke and contaminated water of industries released unchecked. Due to which hazardous gases and particles enter in air, water and soil, and cause poisoning of environment.

- **Population Growth**

Population growth [3] is second fundamental cause of pollution. Population of the world is increasing with a very high rate due to which consumption of different goods increasing, so production rate and use of natural resources are also expanding which in turn causes pollution.

- **Globalization and Urbanization**

Globalization and Urbanization is another major factor of pollution [3]. It causes environmental degradation. Developing countries has cheap labor and weaker laws of environmental protection which facilitate industries, so industries prefer to move such types of areas and cause pollution. Moreover people migrate to big cities because big cities have more opportunities and have better facilities, which results in increasing rate of pollution in major cities.

- **Pollutants and Their Effect on Human Health**

Pollution is a severe threat to human health [3, 7]. Many poisonous chemicals and gases like, , nitrogen oxide, carbon monoxide (CO), carbon dioxide (CO_2), chlorofluorocarbons, sulfur dioxide etc are released unchecked into our environment, which causes air pollution. Air pollution has a devastating effect on human health [8]. Many air born diseases e.g. lung cancer [9], asthma, allergy and breathing problems are arising. Industrial wastes release different chemicals such as paints, dyes, detergents, fertilizers and heavy metal particles, which causes water pollution. Diarrhea, malaria, dengue [3], hepatitis, cholera, typhoid fever, HIV/AIDS and many more diseases are arising due to water pollution.

The soil is polluting due to oil spills, high use of fertilizers and pesticides, dumping off non-degradable garbage, salts and radioactive elements. These hazardous chemicals are affecting the life and growth of plants and also causing serious diseases in humans e.g. cancer, kidney and liver diseases, skin infection, nervous system damage etc.

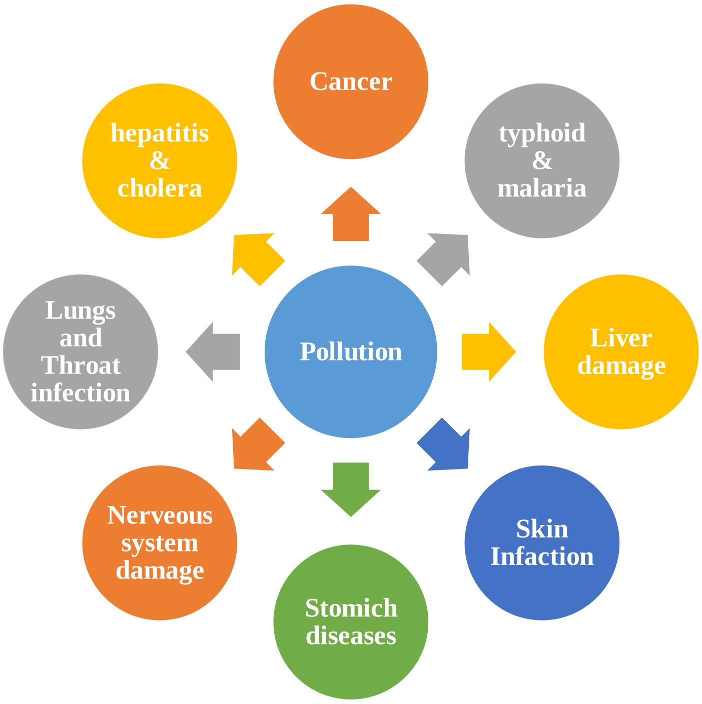

Figure 1.2. Diseases caused by pollution

1.2.2 **Energy Crisis**

In recent years a lot of attentiveness is being paid to the issue of energy crisis and energy security because it is a severe problem worldwide [4]. The Energy demand of the world is is increasing rapidly so production of energy is also increasing but the production rate is lower than the demand, which leads to the energy crisis. Going to the other factors of energy crisis we have to talk about the fossil fuel which is used as the source of energy throughout the world from centuries and the risk of its depletion is becoming major fear of the world.

- **Fossil Fuels, Fundamental Source of Energy**

Most of the world's energy is produced by conventional ways [7], which uses vast but finite natural resources, like coal, gas and petroleum. Due to higher demand, the extraction of fossil fuels and production of energy from them reaches to its peak. It is a serious threat that natural fuels are depleting at very high rate and shortage of fossil fuels get the modern world back to its feet so it is need of the hour to shift towards the energy resources that are renewable.

A report was published in 2008 [10], which stated that natural resources are the main contributor of global energy production (Nuclear energy 2 %, Oil 36 %, Coal 28 %, and Gas 22.%) and renewable energy resources just contribute little (only 12.9%).

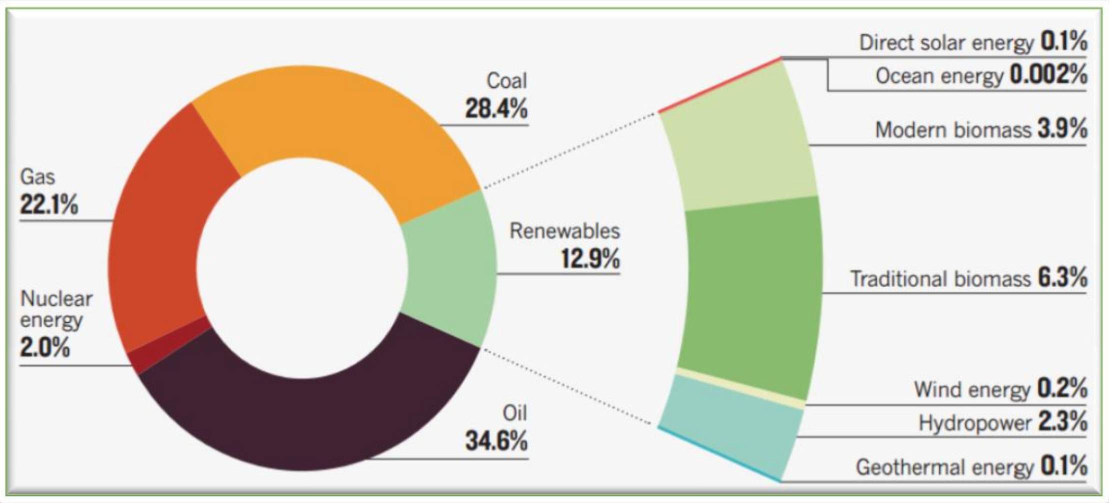

Figure 1.3. Sources of energy production [Adapted from Ref. 11]

- **Advantages of Fossil Fuels**

Modern age is an age of industrialization and globalization, to meet the requirements of modern society, fossil fuels are man's best friends because they have many advantages over the others e.g.

- They are very stable due to the presence of highly stable carbon and hydrogen molecules.
- They produce greater amount of energy on combustion.
- They have high calorific value so they have higher efficiency over other types of fuel.
- Due to the advancement in science and technology extraction and refinement of fossil fuels become easy due to which fossil fuels are readily available throughout the globe.
- Their transportation and storage capabilities are easy due to high stability.
- Fossil fuels are abundantly available in every part of the world.
- They are cost effective.
- Setting up of power plants and refineries of fossil fuels are easy and can be made anywhere in the world.

- **Limitations of Fossil Fuels**

Fossil fuels have many advantages as discussed above, but they have some serious limitations which are alarming for the world, and these limitations make us think to some alternative energy resources. Some of the highly concerned limitations of fossil fuels are listed below,

- They have serious environmental concerns because burning of fossil fuels release some highly dangerous gases which cause environmental pollution and global warming e.g. carbon dioxide.
- Burning of fossil fuels also release sulfur dioxide, which is the source of acid rain; and acid rain leads to the destruction of crops, marble-made buildings, brickwork, and also causes some serious diseases of respiratory system.
- Ozone depletion is caused by green house gases which are also released in our environment by the burning of fossil fuels. It results in the formation of holes in ozone layer, and dangerous UV rays enter the earth surface, which causes cancer and other skin diseases.
- Fossil fuels are transported from one part of the world to the other by different means e.g. by air, road or sea, and if some accident or shrinking of oil occur during transportation, it can cause serious problems e.g. oil spills in water can harm the aquatic life in very serious way because crude oil contain very hazardous chemical.

- Depletion of fossil fuels is the biggest concern. Fossil fuels have been serving as a source of energy from centuries, but now there is a threat that the higher consumption of fossil fuels will lead to their depletion and after some decades no fuel will remain to fulfill our needs. In future the price of fossil fuels might hike to a very high level due to their limited availability. So it is need of the time that we have to find some renewable energy resources which are not only necessary to fulfill our future needs of energy but also protect our environment from being polluted.

- **Causes of Energy Crisis**

There are various causes of energy crisis which are discussed in detail below,

- **Rapid Industrialization**

From last century, there is a rapid increase in global industrialization, which needs energy for its working and almost 50% of energy is utilized by industries worldwide [7]. Different industries, like agriculture, mining, construction and manufacturing utilize energy. This industrial revolution is the main cause of energy crisis because the demand of energy is increased to a high rate.

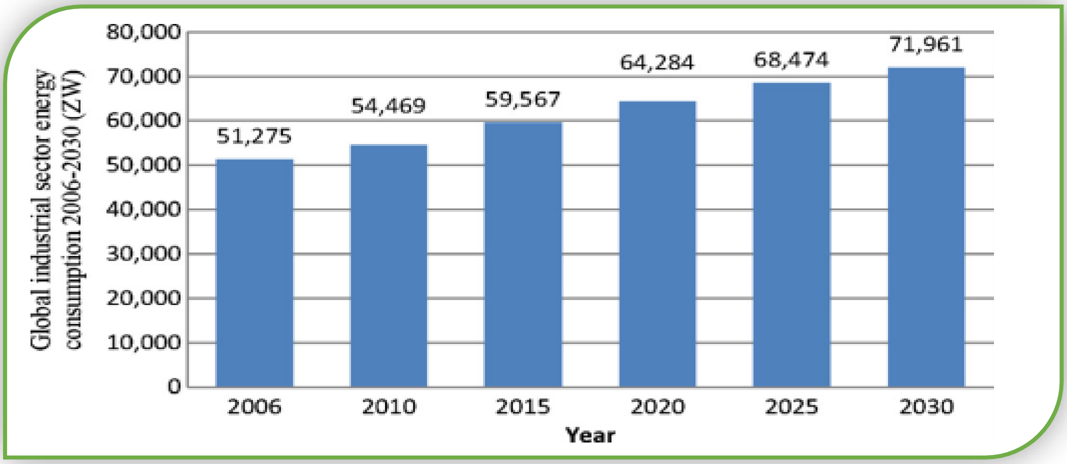

Figure 1.4. Global energy consumption during 2006-2030 [Adapted from Ref. 8]

- **Overpopulation**

It is another major cause of energy crisis. The population of the world is continuously increasing and the demands of products and fuel is also increasing. Every product we use and every food we eat need energy to prepare, transport and trade. So by increase in population, need of energy also increases but sources to produce energy are not increasing at a rate to meet the demands, which results in energy crisis.

- **Wastage of Energy**

Most of the people do not pay much attention to conserve energy. We have to give some serious thoughts to save energy. Simple things like switching extra lights and fans, maximum use of day light, travel small distances by feet and control over the leakage of energy can help to reduce energy crisis.

- **Poor Infrastructure**

Outdated power generation machinery is also another reason of energy crisis. The energy supplying firms are mostly using poor and old fashioned equipment for the production of energy due to which the production power of different power generation plants is low, which leads to the shortage of energy supply, and this condition is severe in developing countries.

1.3 Solutions of the Problems

There are many possible ways through which we can reduce the pollution and energy crisis. Advancement in science and technology can help us in many ways to find out solutions to these severe threats.

1.3.1 **Reduce Personal Consumption**

It is the first step to reduce the pollution and energy crisis. When personal demand increases, level of supply and production also increases, which not only results in the high-level use of energy but also results in the increased level of pollution. We consume different good and products, which release harmful gases like CO_2, CO, chlorofluorocarbons and also produce a high amount of waste and garbage. So if we reduce personal uses, pollution will be reduced definitely and rate of production and transportation of goods also reduces, which can save energy and fossil fuels.

1.3.2 **Recycling and Reforestation**

Recycling can play a key role to reduce pollution. Different things can be recycled and reused easily like shopping bags, paper, tins and bottles. It can reduce pollution and also a rate of production, so not only pollution is reduced but also energy for their production is saved. Reforestation is one of the major solutions to the pollution; it not only maintains the temperature but also prevents from a landscape and reduces carbon dioxide by increasing photosynthesis.

1.3.3 Use Clean and Renewable Resources of Energy

It is the best solution to resolve the issues related to energy crisis and pollution. A detailed discussion of green and renewable energy resources is given below,

- **Biomass**

Biomass is referred as plants or plant based biological material that can be used as bio-fuel to produce energy in the form of heat, as a result of their combustion. Plants make their own food by utilizing sunlight in the process of photosynthesis and reserve this in the form of chemical energy. When plants die this stored energy is converted into biomass energy and can be used as a renewable source of energy. Other forms of energy like biodiesel, ethanol and methane gas etc. can be produced by biomass.

- **Wind**

Wind energy is a type of kinetic energy which is stored in the wind. It is unlimited energy source which can fulfill the global demands of energy, and also it helps to reduce the pollution because it is a green source of energy. Wind cycle is utilized to produce electrical and mechanical energy by wind turbines and wind mills, respectively, and then this energy is stored and transferred by transmission line.

- **Water**

Water contains 71% area of the earth. It is a huge source of energy. Moving water has kinetic energy which can be converted into electrical energy. To generate hydro-electrical energy, water is stored in a dam and this stored water has potential energy. This water flows down with high speed. Flowing water has kinetic energy which run the shaft of the generator and produces electrical energy. Amount of electricity produced by a dam is directly related to an amount of water stored in the dam. The flow of water in a dam is controlled by gates.

- **Geothermal**

A very high amount of heat is trapped inside the earth crust which leads to the formation magma. Magma is molten rock and has a very high temperature. It is preset 1800 miles beneath the surface of the earth, due to very high temperature of magma, rocks near the earth surface are also maintained higher temperature, and this stored thermal energy is used to produce electrical energy. Deep wells are dug and cold water is pumped down, which flows in cracks of hot rocks and converted into steam or hot water, which is pumped out and used to run a turbine and produce electricity.

- **Solar**

Solar energy is the best-known form of renewable energy. It can overcome the interrelated issues of environment and energy. The shining sun contains an immense amount of energy which is almost 100000TW/year, and the need of energy in 2010 was 15-17 TW, and it will increase up to 25-27 TW in 2050. We can attain this energy by converting only 10 % of the solar energy, in 0.3% surface area of the earth.

1.3.4 Introduction of Eco-Friendly and Efficient Technologies

Eco-Friendly and efficient technologies like nanotechnology can help us to reduce pollution and energy crisis. We can use eco-friendly products e.g. cars, eco-friendly energy sources e.g. wind and solar energy, and efficient electrical appliances, recycling of material, as much as possible.

1.4 Nanotechnology

Nanotechnology is a fast growing field of science which deals with the matter ranges from 1-100 nm in size [11], at least in one dimension. It explains properties of matter at atomic and molecular scale. At such a low size range, surface area of matter becomes very high and some interesting phenomena's occur. Properties of nanomaterial differ from bulk material due to which, they have very useful applications and they can be used to solve many issues of the modern world including, issues of health, environmental pollution and energy crisis.

1.4.1 Types of Nano Materials

There are four types of nanoscale material,

- Carbon based nanomaterials
- Metal based nano materials
- Dendrimers
- Composites

- **Carbon Based Nanomaterials**

These nanomaterials are mostly composed of carbon, and they exist commonly in the form of ellipsoids, hollow spheres and tubes. Ellipsoidal and spherical carbon nanomaterials are referred as fullerenes and cylindrical carbon nanomaterials are called nanotubes. The structure of fullerenes is similar to graphite. It is composed of stacked graphene sheets of linked hexagonal rings, but sometimes it may contain pentagonal or heptagonal rings [12]. Carbon nanotubes are cylindrical in shape and their diameter is very small, ranges up to 1 nanometer, but their length ranges to several micrometers [13]. These particles have many applications in electronics. They also served as coating materials and used in the formation of stronger but lighter materials.

- **Metal Based Nanomaterials**

Metal based nanomaterials are composed of nano metals, like silver and gold nano particles, metal oxides e.g., titanium dioxide, and quantum dots. A quantum dot is composed of hundreds of thousands of atoms; it is closely packed and crystalline material. Its size ranges from few to few hundred nanometers, and its optical properties changes if size is changed [14].

- **Dendrimer**

It is a nanoscale polymer made up of numerous branches, having chain ends at the surface. It often makes three dimensional [15] hollow cavities, due to which it can place small molecules into its cavities for specific chemical reactions, like catalysis. It can also be used for drug delivery.

- **Composites**

Composites are made up of different combinations of one type of nano material with other type of nano materials, or with bulk material. Catalytical, thermal and mechanical properties of the nano materials are enhanced by making their composites with other material. Nanocomposites also have improved optical, electrical, magnetic and protective properties, like corrosion resistance [16].

1.4.2 **Synthesis of Nanomaterials**

Nanomaterials possess various applications in many fields e.g. in electronics, medicine, energy and environment. Use of nanomaterials in these fields depends upon their physicochemical properties, like size, morphology and Crystallinity etc. It is an interesting and challenging area of research to develop nanomaterials having desired properties. In a broad view, fabrication of nanomaterials is divided into two main classes *i.e.* top down approach and bottom up approach as given in **figure 1.5.**

- **Top-Down Approach**

In this technique, the bulk material is converted into nanomaterial by a successive breakdown. Physical and chemical properties of synthesized nanomaterials are controlled externally by means of different devices. Mechanical milling [17] is a well-known method of top down approach, to synthesize different types of nanomaterials.

- **Bottom-Up Approach**

It refers to the technique in which nanomaterial is built up step wise, firstly molecular precursor is broken down to atoms then atoms nucleate to produce nanomaterials. Bottom-Up has more advantages over top-down approach due to more control on size and structure; moreover, it is an economically feasible method.

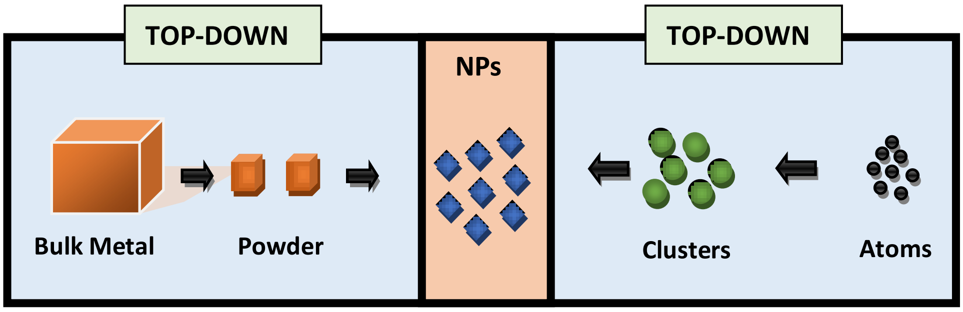

Figure 1.5. Top-down and bottom-up approach for synthesis of nanomaterials

It is further divided into three subclasses *i.e.*

- Liquid phase synthesis
- Vapor phase synthesis
- Gas phase synthesis

In the following discussion, liquid phase synthesis is only under focus. In this method solutions of the precursor are used to fabricate the nanoparticles in a liquid medium, it is further divided into different methods *i.e.* listed at next page,

- Sol Gel method
- Combustion Method
- Microemulsion Method
- Sonochemical Method
- Hydrothermal method

In this context hydrothermal method is discussed in detail because the reported nanomaterials present in next chapters are synthesized by this method; however an overview of other methods is also given below,

- **Sol Gel Method**

In this processes mostly alkoxide precursors are used. It has a stepwise procedure in which firstly liquid phase "sol" is synthesized and then converted into solid like "gel"; after drying the gel is annealed. Properties like size and morphology etc. of synthesized nanomaterial are controlled by controlling pH of solution and reaction temperature [18]. Sol-gel method has an advantage that it requires lower temperature for annealing, but the requirement and of the longer time for drying of the gel is its limitation.

- **Combustion Method**

This method requires rapid heating of precursor solution at very high temperature *i.e.* up to 650 $^{\circ}$C, in the presence of redox group [19]. The synthesized product has large surface area and high crystallinity, due to high temperature [20, 21].

- **Microemulsion Method**

High quality nanoparticles with small size can be produced by this technique. Microemulsion [18] is defined as "it is a thermodynamically stable and isotropic dispersion system, of two immiscible liquids" e.g. oil and water. Surfactants with a concentration greater than critical micelle concentration are also used here.

- **Sonochemical Method**

It is a different method as compared to other conventional methods because it uses ultrasound waves having high intensity. It does not require high temperature and high pressure. This method is based on the phenomenon of acoustic cavitation (*i.e.*, the formation, growth and implosive collapse of bubbles) in liquid. Severe momentary conditions of ultrasound waves result in the formation of hot spots which can acquire a temperature up to 5000 K and pressure up to 1000 atm and heating, cooling rates around 10^{10} KS^{-1} [22, 23].

- **Hydrothermal Method**

The word hydrothermal is a sum of two words “hydro” and “thermal” which means water and heat, respectively. The term hydrothermal was firstly used by a British geologist named Roderick Murchison, who said that “at elevated temperatures and pressure there is a specific action of water which bring changes in the earth crust and produce certain minerals” [24]. Hydrothermal method is defined as, “it is a reaction in which aqueous or non-aqueous solvent is used for the synthesis of nanoparticles, it is carried out at temperature higher than room temperature, and pressure higher than 1 atm”. Most of the material scientists say that required temperature is greater than 100 ^{0}C [25].

At elevated temperature and pressure the chemical properties of different precursors, like solubility and reactivity changes, and dissolved precursors are recrystallizes in a liquid medium. Due to efficient control over conditions, like reaction time, temperature and concentration of precursors, high-quality nanoparticles with uniform size distribution are obtained.

In the hydrothermal method, a precursor solution is added in a non-corrosive teflon/carbon tube, which is placed in a stainless steel vessel called autoclave, which can bear conditions of high temperature and pressure. The autoclave which acts as a reactor in this method, is completely closed and putted in an oven at desired temperature due to rising in temperature, pressure is also rose which leads to the formation of nanoparticles.

Over other methods of synthesis hydrothermal method has certain advantages that are given below,

- Hydrothermal is economically feasible and cheap method because the respective cost of energy, instrumentation and precursors is less.
- It is environment-friendly and safe method due to the use of tightly sealed autoclave, in which whole of the reaction takes place.
- Temperature requirement for this method is also low as compared to other methods.

- It gives higher command over reaction temperature and time which results in better control over size and morphology of synthesized nanomaterial.

1.4.3 Properties of Nanomaterials

- **Dimensional Properties**

Materials show different properties in nano regime as compared to their bulk form, due to two main factors *i.e.*

(a) High Surface to Volume Ratio

There is a well-known relation *i.e.*

$$\text{Surface to volume ratio} \propto 1/\text{size}$$

At nano scale dangling bonds increases, which results in enhanced reactivity and surface properties.

(b) Quantum Size Effect

In bulk form, materials have continuous energy level but in case of nano form, energy levels are quantized because electronic wave function becomes confined to the physical dimensions of nanoparticles [26].

- **Optical Properties**

Optical properties of nanomaterials and their bulk correspondents are quite different from each other due to the following effects,

- Quantum confinement effect
- Formation of discrete band gaps
- Meager material effect
- Surface Plasmon
- Formation of surface states

Metals show interesting behavior in nano regime due to the formation of band gaps, *i.e.* they are converted to semiconductor and insulator, from conducting material. When the size of a metallic material, like ZnS coated CdSe is reduced, it shows blue shift [27] as shown in the **figure 1.6.**

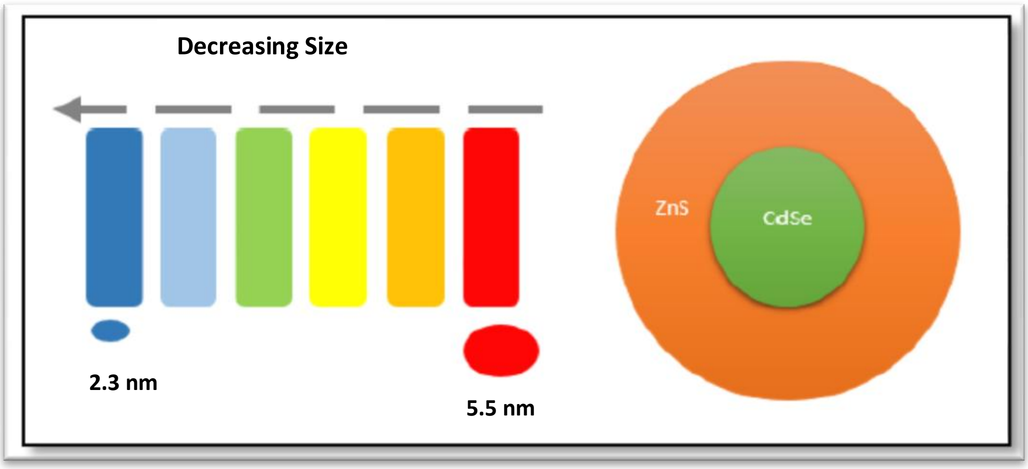

Figure 1.6. Appearance of blue shift due to reduction in size in CdSe quantum dot

- **Electrical Properties**

Now a day Nanomaterials are highly used in different technologies due to their suitable electrical properties [28]. Electrical properties, like conductivity, resistivity, thermoelectricity and dielectric strength of nanomaterials are very suitable for different applications.

- **Catalytical Properties**

We can divide the catalytic properties of nanomaterials into two major classes: *i.e.* electro-catalytic properties or electro-catalysis and photo-catalytic properties or photo-catalysis.

- **Electrocatalysis**

It is a type of catalysis in which the surface of electrodes or electrodes itself are made up of semiconductor nanomaterial, which acts as a catalyst. Its catalytic activity is initialized by passing the electricity through the system. Electrons are generated, which may result in an oxidation-reduction reaction, oxidation occurs at an anode while at cathode reduction takes place [29].

Nicholson, in 1800 worked at water electrolysis, and after 1900 this work gained much attention due to industrial revolution [30]. By water electrolysis, water molecules can be splitting into individual hydrogen and oxygen atoms. High voltage of electric current is used in this method and as result hydrogen (a green) can be produced which is a green fuel. Electrocatalysis can also be used for waste water treatment.

- **Photocatalysis**

Semiconductor photocatalysts have gained much attention during last three decades due to their applications in energy and environment. Since, the work of Fujishima and Honda [31] *i.e.* photo-electrochemically water can be split into hydrogen and oxygen by titanium oxide, under UV light. Titanium oxide is a semiconductor photocatalyst.

- **Mechanism of Photocatalysis**

Electrons are present in valance band of semiconductor nanomaterial and when light is irradiated they got excited and migrate to conduction band in this way holes are left behind, in valance band. There is a chance of the recombination of generated charge carriers. If the recombination may be reduced then these electron-hole pairs can be used for different oxidation reduction reactions, with organic and inorganic species; which results in increased photocatalytic efficiency.

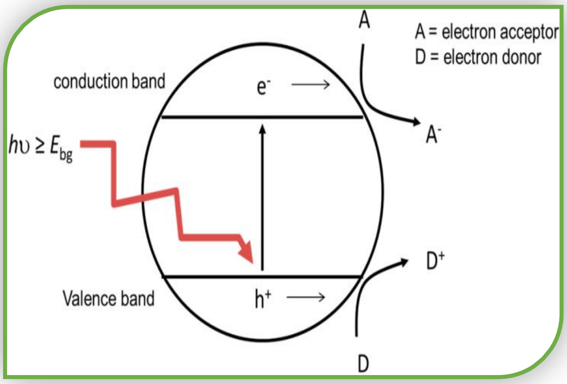

Figure 1.7. Mechanism of photocatalysis

- **Methods for Improved Photocatalytic Efficiency**

Photocatalysis is an effective method for the degradation of organic wastes like CO_2, organic dyes and it is also used for waste water treatment, but the efficiency of semiconductor based photocatalysis is low, due to electron-hole recombination. Different researchers have worked to overcome this problem. Here some strategies are given which can improve the photocatalytic activity of inorganic based semiconductor photocatalysts.

Band Structure Engineering

It is a good method to improve the photocatalytic activity of a material. It has different strategies, like quantum confinement effect, doping, solid solution, sensitization and hetero structuralization.

Quantum Confinement Effect

Due to its efficient charge separation and effective solar light absorption activity, quantum confined semiconductor nano crystals have improved photo-catalytic activity [32-34]. They have large extinction coefficient and longer life time. These quantum confined photocatalysts have improved photo-stability and having a possibility to generate multi-electrons by single photon [35].

Doped Semiconductors

Anion doping: Recently different metal oxide semiconductors have been synthesized with band gap around 3 eV [36]. They have good catalytic efficiency, but the work only under UV light. We can bring their photocatalytic activity to the visible part of the solar spectrum by doping with different anions, like carbon (C), fluorine (F) and nitrogen (N) [37-39].

Cation doping: We can improve the photocatalytic activity by doping it with a cation, like Cu [40, 41], Ni [42, 43], Ag [44, 45], Au [46] and Nd [47]. By cation doping recombination is reduced and it also shifts the absorption range from UV to visible region, because "impurity band" is formed within the band gap of the photocatalyst.

Sensitization of Semiconductor Photocatalyst

Large bandgap semiconductor photocatalysts, like metal oxides, show their photocatalytic activity in UV region of the solar spectrum which is only 4%. Hence, to bring their photocatalytic activity to the visible region, wide band gap semiconducting

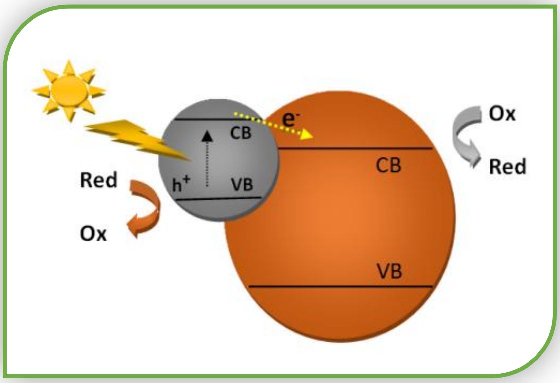

Figure 1.8. Sensitization of photocatalyst

photocatalysts are sensitized by narrow band gap semiconductor, or with a dye, as shown in **figure 1.8**. The photogenerated electrons are migrated from conduction band of dye or narrow band gap semiconductor to the conducting band of wide band gap semiconductor, in this way recombination is reduced. The best example of sensitization of photocatalyst is sensitization of TiO_2 with small bandgap semiconductors, like CdS [48], quantum dots of CdSe and PbS [49, 50], and different dyes like, Cu (I), cobalt-phthalocyanine and zinc-phthalocyanine are used, which brings the absorption range of TiO_2 to visible region.

- **Development of Hetero-Structures**

It is also a promising technique to enhance the photocatalytic efficiency. The photocatalytic activities of ZnO/ZnSe [51], nitrogen-doped graphene/ZnSe [2011], and $Co_3O_4/BiVO_4$ [52] hetero-structures, are higher as compared to individual nanomaterial. It provides better charge separation, due to the transfer of electrons from higher to a lower conducting band, and holes from lower to the higher valence band, as shown in **figure 1.9.**

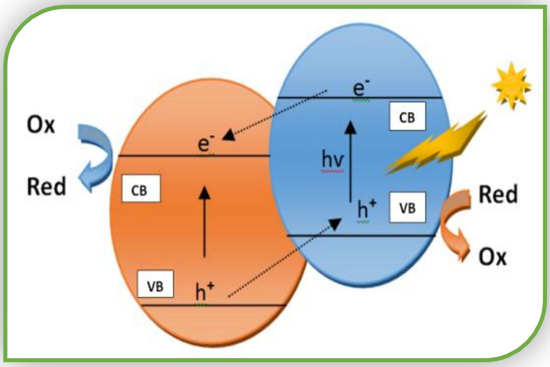

Figure 1.9. Heterostructure for photocatalysis

- **Formation of Porous Structures**

Porous structures can act as good photocatalysts, because they have improved physical and surface properties due to the presences of a large number of channels e.g. porous ZnO/ZnSe nanocomposite [53] and porous Co_3O_4 [54, 55] show improved photocatalytic activity.

- **Nano Structuralization**

Formation of nanostructures of different morphologies e.g. nanowires, nanorods [56] and nanobelts [57] etc., is also a promising technique to improve photocatalytic activity because they are single crystalline materials and they lack the charge recombination centers *i.e.* surface defects, so the chances of recombination are less in these materials.

- **Cocatalyst**

Cocatalyst assisted photocatalysis is one the best and highly researched method, in this method Schottky barriers, are formed between cocatalyst and semiconductor, which reduces the recombining of electrons and holes [58], as shown in **figure 1.10**. Different metals nanoparticles including Au [46, 59], Ag [60-62], Rh [63] and Cu [64, 65] are used as cocatalyst because their fermi level is located just beneath the conducting band of semiconductor nanomaterial. Hence, the electrons are easily shifted from semiconducting nano photocatalyst to the cocatalyst, and electron-hole recombination is reduced.

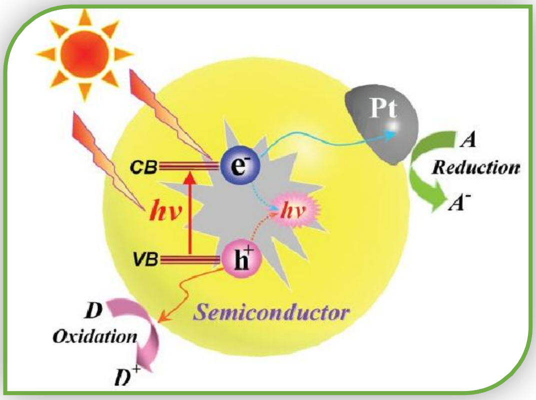

Figure 1.10. Cocatalyst assisted photocatalysis [Adapted from Ref. 58]

1.4.4 Applications of Nanomaterials

Nanotechnology is revolutionizing the modern world; it has many applications and benefits in the fields of medical, food safety, homeland security, information technology, everyday materials, transportation, environmental sciences and energy sector.

- **Everyday Materials and Processes**

Nanotechnology is helping material sciences to make more reliable, durable, stronger and lighter materials which are more beneficial to mankind.

- Nanotechnology helps in the field of polymer and nanoscale additives in bike helmets, bumpers of cars, tennis rackets and baseball bats etc. make them stronger and light weight.
- Fabric industry is revolutionized by the nanotechnology, wrinkle free, light weight and more durable fabrics are made.
- Coating of nanoscale thin films on glass of windows, display of camera and computer, and on eyeglasses, made them water repellent, self-cleaning and scratch resisting and resisting to ultraviolet and infrared radiations.

- In cosmetic industry, nanoscale materials are added in creams, shampoos and lotions. They are used in specialized makeup, which gives better cleansing and clearness and also, they are used in complexion treatment. Nanomaterials give better health properties because they work as antimicrobial and antioxidant.
- In food industry different nanocomposites are used in packaging of different beverages, to prevent oxygen inflow; carbon dioxide and moisture outflow. Different types of nanosensors are used to detect contaminated food. Nanomaterials are also used as antibacterial agents who keep food safe and fresh for longer time.
- Nanoscale materials are used in paint industry to make paints more resistant to harsh environmental conditions. They are also used in cleansing industry to clean fabric leather etc.

- **Applications in Electronics and Information Technology**

Nanotechnology has vital applications in data storage, data transmission, and communication and computing.

- Now a day nanoscale transistors are in use which is more energy efficient, faster and powerful. Magnetic random access memories (MRAM) are also used which contain nanomaterials and give better data storage and data recovery.
- An organic light emitting diodes (OLED) are used in a display of a computer, television and camera which give better picture quality, wide angle range has a longer lifetime and consumes low power.

- **Nano Bio-Systems, Health and Medical Applications**

Nanotechnology has potential to revolutionize the fields of medicine and biotechnology. Its applications give safer, cheaper and more reliable results in the medical field.

- In the field of biological imaging, quantum dots are used, which are nanoscale semiconducting materials. They give better resolution so diagnosis by medical imaging becomes more reliable when quantum dots are used. They give 1000 times better detection than conventional tests, such as Magnetic Resonance Imaging (MRI) which uses normal dyes in testing.
- Nano particles of gold are used to detect Alzheimer’s disease at early stages.

- Nanotechnology is used to treat cancer cells, preventing the risk to damage or effect normal cells.
- Advance research is in progress in medical field to cure damaged nerve cells and spinal cord with the help of nanomaterials.

- **Advanced Transportation Applications in Future**

- Nanotechnology is used to make “green” vehicles, air craft’s and ships which are more reliable, fast, cost effective and lighter.
- A nanoscale material is used in steel and cement industry which gives more strength to them, and when these cementitious materials are used in roads, it gives longer lifetime and greater strength to roads and high ways, while reduces cost.
- By the advancement in nanotechnology, scientists and engineers are able to make different sensors which can be used to monitor performance and strength of tunnels, bridges, pavements and railways tracks continuously, and help to control from damage and accident.

- **Applications in Renewable Energy**

Renewable energy means “production of light, electricity and heat without polluting the environment”. Nanotechnology has vast applications in the field of energy. It is not only used to produce renewable energy but also the materials made up with the help of this technology have very short energy demands due to very small size.

Advantages of nanotechnology in the field of energy are given bellow,

- Material made up by nanotechnology has higher efficiency in heating and lightning.
- Energy production and usage, is environment friendly when it is done with the help of nanotechnology.
- Nanomaterials have higher electrical storage capacity.
- Nanotechnology is also used to increase the efficiency of other energy sources, e.g. nanomaterials are used to make rotor blade, which is stronger and lighter and used in the production of wind energy. Nanocomposites are used as coating agents on the drilling machines, used in geothermal energy production, for making them stronger and fatigue resistant. Nanomaterials are used for the coating of equipment used in tidal energy production process and prevent them from corrosion.

In energy storage and sustainable energy production, nanotechnology has advantages that are described below,

- By the use of nanotechnology, the energy production rate and energy storage, in a photovoltaic cell are increased and production cost is reduced.
- In fuel cell by the use of nanomaterials, hydrogen production, hydrogen storage and its transformation into electricity is being increased, because by the use of nano materials, hydrogen absorption capacity of fuel cell is increased and also it become cost effective.
- Hydrogen which is a green fuel now can be synthesized by nano photocatalysis [66-68] which may help to full fill the energy demands in near future without polluting the environment.

- **Environmental Applications**

Beside from the production of cars, truck and heavy machinery with a light weight nanomaterial, which needs less fuel and hence, cause lesser pollution, nanotechnology also has many ecofriendly applications. Green fuel is produced with the help of nanotechnology which is environment friendly. Many nanoparticles are directly used to reduce pollutants from air and water, and also used to mitigate global warming.

- Nano zero valent iron (nZVI) is used to remove pollutants such as chlorinated solvents e.g. tri and tetrachloroethenes, and also used to eliminate heavy metal particles [69, 70]. Iron is cheap and abundantly available so it is a good reductant of many compounds, but nano zero valent iron made a thin coating of iron oxide when placed in water, which limits its activity.
- Nanoscale silver is used in desalination membranes, which are being used to convert saline water and seawater to potable water. Many nanoscale particles are used in catalysis e.g. TiO_2. TiO_2 is used to oxidize many pollutants in water, which includes undesirable organic wastes, pharmaceuticals, pesticides petroleum byproducts, inorganic compounds like ammonia [71, 72]. TiO_2 also used to remove pollutants from air, and thin membrane of TiO_2 is used in water bottles to remove pathogens from drinking water.
- Nano ceria (CeO_2) is used as catalyst in water gas shift reaction. It is also used in the process of ammonia production [73, 74]. CeO_2 also used to reduce the energy required for the production of ammonia [75], and hence reduce the emission of

pollutants. Emission of hydrocarbons from internal combustion engine is also reduced by the use of CeO_2 nanomaterials [76, 77].

- Nanoscale materials are also used as absorbent of different pollutants of air and water e.g., carbon nanotubes, which can absorb many organic and inorganic hazardous compounds [78, 79].
- CO_2 reduction is done by photocatalysis, which is a property of semiconducting nanomaterials, it not only helps to reduce pollution but also used for the production of fuel like CH_4 [80, 81].
- Different organic dyes e.g. rhodamine B [82], methyl orange [83] and congo red [84] are degraded by nano photocatalysts in the presence of UV-Visible light. In this way organic dyes are removed from water, which are the main cause of water pollution.
- Nanotechnology is also used for the cleaning of oil spills, nanowires of potassium manganese oxide are used for this purpose. This method has an advantage, that oil is recovered, and these nanowires are also reusable.

1.5 Characterization Techniques

Synthesized sample was characterized by following techniques,

- X-ray Powder Diffraction (XRPD)
- Scanning Electron Microscopy (SEM)
- UV-visible Spectroscopy
- Energy Dispersive X-ray Spectroscopy (EDS)

1.5.1 X-ray Powder Diffraction

X-ray powder diffraction (XRPD) is a promising technique to identify, crystallinity, phase and unit cell structure of a material. It gives detailed information about the crystal structures, cell volume, lattice constant and crystallite size.

- **Principle**

A beam of X-ray is fall on the material and electronic cloud of that material scatters the beam in different directions and constructive interference occurs. If the separation between the material's atoms and wavelength of directed X-rays are comparable then the constructive interference resulted. Bragg’s law must be obeyed during this process, which is described as:

$$n\lambda = 2d\sin\theta$$

where,

λ = wavelength of incident light.

θ = diffraction angle.

d = line spacing (Inter atomic distance).

Parts of X-ray Diffractometer

Following are the main parts of X-Ray Diffractometer:

- X-ray tube (T)
- Filters (F)
- Beam slits (BS)
- Beam masks (BM)
- X-ray mirror (A)
- Monochromator (M)
- Sample holder (S)
- Detector (D)
- Display unit (B)

Figure 1.11. XRD machine

Mostly, Cu LFF X-ray tube is used with high transmission (94%) of Cu K_α X-rays. A filter (F) sometimes is used which suppresses the K_β radiations. The role of beam slits (BS) is that, they control the equatorial divergence of beam coming from X-ray tube. beam masks (BM) are used to control the axial width.

The X-ray mirror (A) is fitted for the diffraction of characteristics K_α radiation. The monochromator (M) is used to improve the resolution. It is fitted between the sample and X-ray tube. Usually aluminum made sample holder (S) is used to hold the sample. The detector (D) of X-ray diffractometer consists of Xenon/Methane gas filled chamber and measures the intensity of diffracted beam. Results are observed by the last part of the X-ray diffractometer, which is a display unit (Computer screen). Schematic diagram of X-ray diffractometer is represented in **figure 1.12**.

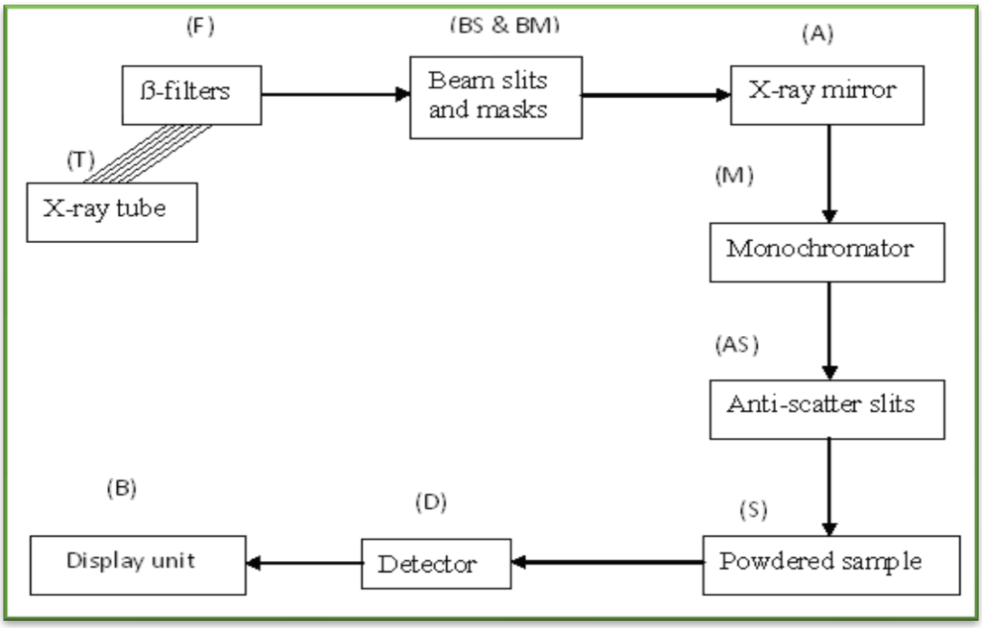

Figure 1.12. Schematic diagram of X-ray diffractometer

- **Pros and Cones of X-ray Diffraction**
- **Pros**
- XRD is a powerful and fast technique.
- It gives clear results.
- A small amount of sample is required.
- Sample preparation is very simple.
- Data obtained by XRD is easy to interpret.
- **Cones**
- A sample must be single phase and homogeneous.
- It needs a standard reference file of all compounds.
- Some time overlapping of peaks occurs and disturbs the results.
- A sample must be ground in powder form.

1.5.2 Scanning Electron Microscopy

In Scanning Electron Microscopy (SEM), samples surface is scanned by a high energy electron beam, in a raster scan fashion. By the interaction of electron beam and atoms present in the sample, information about the topology, morphology and composition is obtained.

- **Parts and working of Scanning Electron Microscope**

Parts of Scanning Electron microscope are listed below,

- Electron gun
- Condenser lens
- Deflection coils
- Sample holder
- Detectors

- **Working**

In a typical SEM usually a tungsten cathode is used because its vapor pressure is low, it is cost effective and having high melting point. An electron gun is attached to the tungsten cathode, which emits electron beam of energy ranging from 0.5 KeV to 40 KeV. Pair of condenser lenses is used to focus the electron beam on a spot, ranging from 0.4 nm to 5 nm in diameter. An electron beam is deflected to X and Y axis by using a pair of deflection plates, which makes raster scanning possible over a rectangular area of the sample surface. Schematic diagram of SEM machine is given at next page, **figure 1.13.**

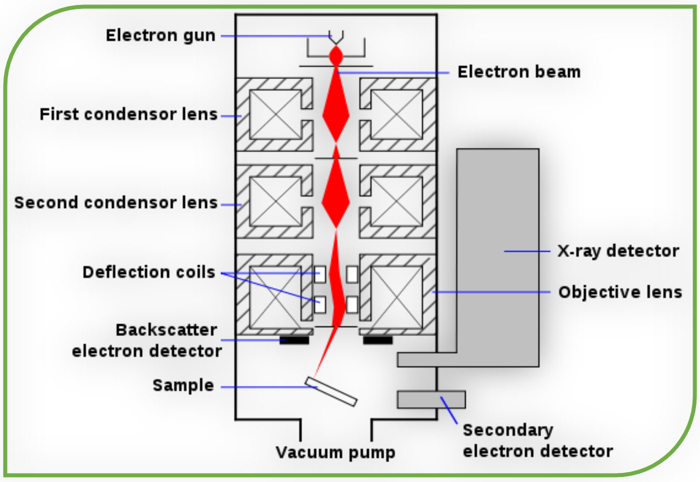

Figure 1.13. Schematic diagram of SEM

When electron beam interacts with the sample, energy is exchanged between them, which results in the emission of electromagnetic radiation, secondary electrons and backscattered electron, by inelastic and elastic scattering, respectively. These signals are detected by specialized detectors, which create an image of the sample and display it on a computer screen.

1.5.3 Energy Dispersive Spectroscopy

It is an excellent technique for elemental analysis and used as an extension to SEM, TEM or XRF. Emitted X-rays are used for the detection of elements which act as finger prints because each element has its characteristic X-rays.

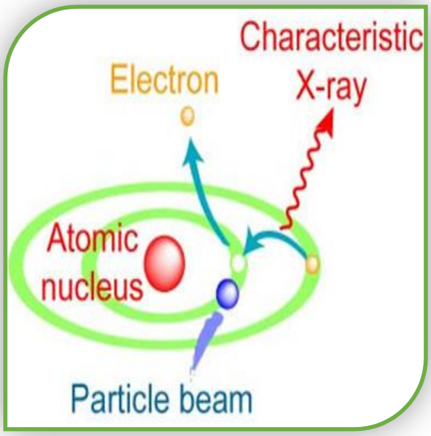

Figure 1.14. Emission of X-rays [Adapted from Ref. 94]

- **Principle**

When a high energy beam is bombarded on an atom, certain elastic and inelastic collations occur between the beam and the electronic cloud, which may result in the knockout of interior electrons. These vacancies are filled by higher state electrons and resulted in the emission of characteristic X-rays [88].

- **Parts and Working of EDX**

There are four major parts of EDX

- Source (electron beam or X-ray beam)
- Detector
- Pulse processor
- Analyzer

There are two types of sources used in EDX *i.e.* electronic beam and X-rays, an electron beam is used in SEM or TEM while X-ray source is used in XRF. The detector of EDX has three parts *i.e.* a sensor, which senses the upcoming X-ray, a preamplifier, which converts X-ray energy into a voltage, then the signal is measured by pulse processor and send to computer for further analysis and display. Schematic diagram of EDX is shown at next page,

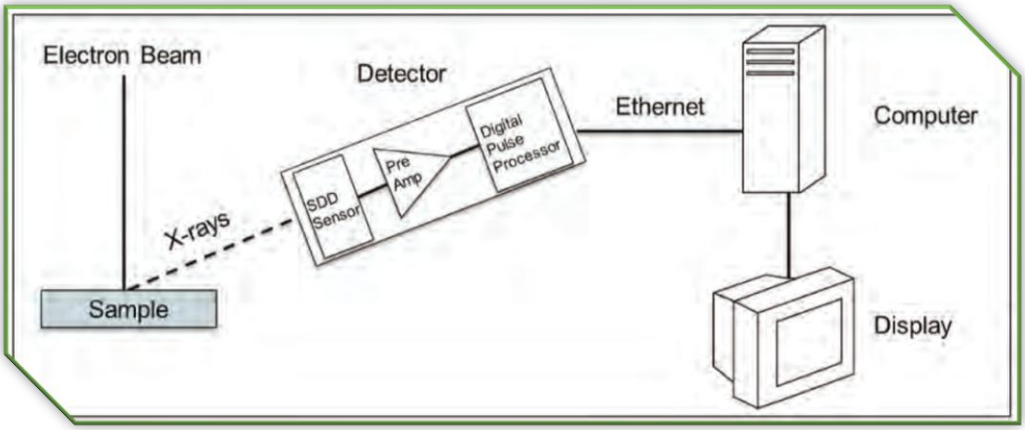

Figure 1.15. Schematic diagram of EDX

- **Advantages and Disadvantages of EDX**
- **Advantages**

- We can identify all elements ranging from atomic no 4 to 92 (Be to U).
- Mostly used as an extension to SEM, so no separate large setup is required.
- The analysis is fast
- Interpretation of spectra is easy and spectral resolution is also good.

- **Disadvantages**

- It only gives atomic information and doesn't give any molecular information.
- Having limited sensitivity to concentrations level on the order of 0.1% in the sampled volume.

1.5.4 **UV-VIS Spectroscopy**

It is a very convenient technique to measure the attenuation of the light beam after it passes through the sample. Sometimes it is referred as absorption spectroscopy.

- **Principle of Absorption Spectroscopy**

Absorption spectroscopy works on the Beer Lambert's law, according to which, the absorbance of light is dependent upon various factors like type of the sample, nature of the absorbing molecules and their concentration. Following relation is used to calculate absorption,

$$A = \log I / I_o \ldots\ldots.. (2.1)$$

where,
A = Absorbance
I = intensity of transmitted light
I_o = intensity of incident light

- **The origin of absorptions**

In any species the valence electron can be present in three types of electronic orbitals,

- Single or σ bonding orbital
- Double or triple bond (π bonds)
- Nonbonding orbitals (lone pair)

The order of energy of these orbitals and the type of possible transition is shown in **figure 1.16**. The mode of transition depends upon the type of material under consideration.

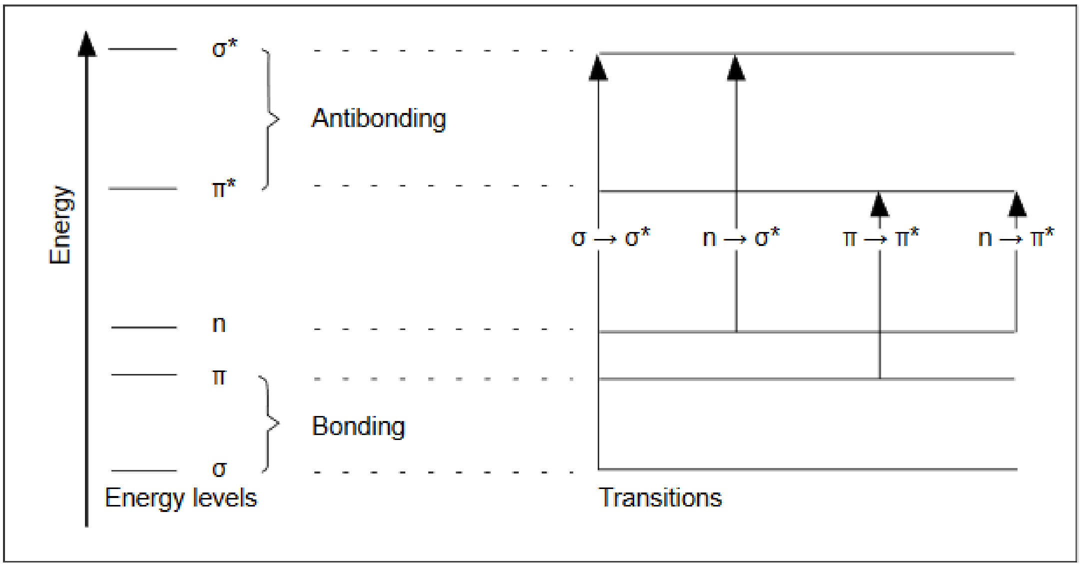

Figure 1.16. Energy of the orbitals and modes of possible transitions

- **Working of UV –VIS Spectroscopy**

Mainly, it consists of a light source, monochromator, sample holder, detector and computer software or data output. A polychromatic light is converted into monochromatic with the help of a monochromator. This monochromatic beam gets converted to transmitted beam after passing through the sample. The transmitted beam is detected by the detector and the results are produced by a computer attached to the spectrometer. The schematic diagram of the working of a spectrophotometer is shown in **figure 1.17.**

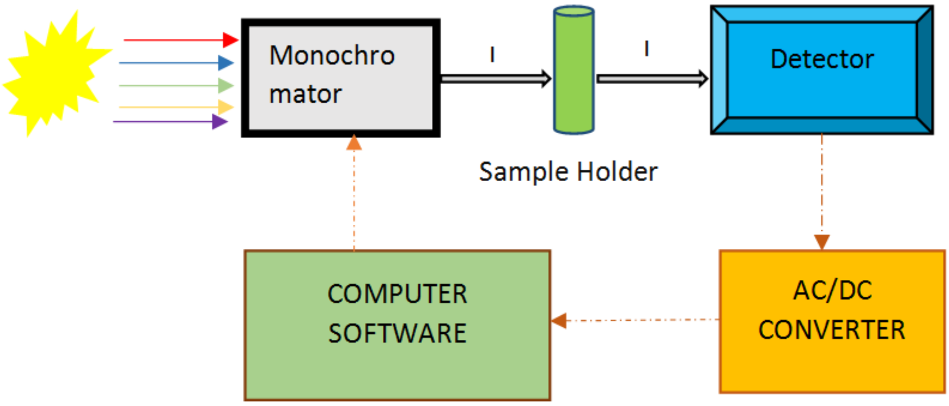

Figure 1.17. Schematic diagram of UV-Vis spectrophotometer

1.6 Photocatalytic Activity

The Photocatalytic activity of synthesized ZnSe, CoTe, Co_3O_4 nanoparticles and Co_3O_4/CoTe, Co_3O_4/ZnSe nanocomposite was measured by degrading Congo red dye, under UV-Visible light irradiation. Xe arc lamp having a UV cut off filter was used as light source for the photodegradation of Congo red dye. With the help of UV-Visible spectrophotometer lambda max was calculated

Xe arc lamp was fitted to 15 cm above the glass vessel of capacity 250 mL, which contain the solution of Congo red dye and catalyst. In the first experiment only dye solution was irradiated and in second experiment a solution of dye and catalyst was made, but no degradation is observed and there was no loss of spectral intensity of the dye has seen in above-mentioned experiments because they are blank experiments.

In third experiment 100 mL solution of Congo red dye was made and 100 mg of catalyst was added to it, under continuous stirring for 15 min, under dark conditions, which ensured the equilibrium establishment between aqueous dye solution and catalyst powder. After the 10 min irradiation, about 5 mL of the dye-photocatalyst suspension was taken out from the reaction vessel and centrifuged to check out the degradation activity. The change in concentration of Congo red dye was measured by measuring the absorbance at λ_{max}. A graph of dye concentration as a function of irradiation time was made, by the help of UV-visible spectrophotometer. Hence, the photocatalytic activity of the sample was measured in this way.

1.7 Scope of This Work

Due to increasing level of energy demands and increasing rate of pollution, it is indeed need of the hour and a challenging task to produce a best possible solution. This work addresses these two problems directly and gives one of the best solutions, by means of photocatalysis.

In the present work, different composites of Co_3O_4/ZnSe and Co_3O_4/CoTe are synthesized and applied for the degradation of organic dye “Congo red” under UV-Visible light. According to best of our knowledge, these composites are first time synthesized and used for organic dye degradation.

Co_3O_4 is p-type semiconductor with band gap 2.07 eV [52] while the bandgap of CoTe is 2.05 eV [85]. ZnSe is an intrinsic semiconductor with band gap 2.7 eV [86]. So, the nanocomposites *i.e.* Co_3O_4/CoTe and Co_3O_4/ZnSe provide a good opportunity to avoid electrons and holes recombination, in this way the photocatalytic efficiency and stability is enhanced.

Chapter 2: Experimentation

Experimental Details

Experimentation includes the synthesis of Cobalt oxide (Co_3O_4), Cobalt telluride (CoTe), Zinc selenide (ZnSe) nanoparticles, and their composites, with different ratios by weight. Synthesis detail is described below,

2.1 Hydrothermal Synthesis of Co_3O_4 Nanoparticles

Hydrothermal method is a wet chemical technique, in which aqueous solution of constituent substances is made. Hydrothermal is an economically feasible method, which gives better control over temperature and time. Hence, command over size and morphology of nanoparticles also increases, as discussed earlier in the first chapter. The autoclave and teflon tube used in the hydrothermal method are shown in **figure 2.1.**

Figure 2.1. Autoclave and Teflon tube

- **Procedure**

A very modest protocol is used for the synthesis of Co_3O_4 nanoparticles [87]. In the **table 2.1** the details of precursors used in this protocol are mentioned.

Table 2.1: Details of chemicals used

Sr. No.	Chemical Name	Chemical Formula	Molar Mass (g/mol)	% Purity	Supplier
1	Cobalt-Chloride Hexahydrate	$CoCl_2.6H_2O$	237.93	98	Panreac
2	Urea	CH_4N_2O	60.06	99.5	Uni-Chem

First of all, 30 mL solution of 0.36 g $CoCl_2.6H_2O$ and 0.72 g Urea is made in distilled water, by continuous stirring then this solution is placed in a Teflon tube, with capacity 40 mL, which was put into an autoclave and autoclave was closed tightly with the help of rod, and placed inside a heating oven for 20 hours at 120 °C temperature. After 20 hours autoclaved is moved out from the oven and cool down to room temperature under normal atmosphere, pink precipitates of $Co(OH)_2$ were obtained, which were washed with distilled water and ethanol, respectively. Then this product is dried over night in vacuum oven. Dried samples were placed in a furnace for 2 hours at 300 °C at heating rate 2 °C/ min. Black powder of Co_3O_4 is obtained at the end, which was ground and stored for further characterizations, and for making different composites, as shown in **figure 2.2.**

2.2 Hydrothermal Synthesis of ZnSe Nanoparticles

Details of the synthesis of ZnSe are given below,

- **Procedure**

The new protocol is developed for the fabrication of ZnSe, *i.e.* similar to the protocol followed for the Co_3O_4, except that annealing in the furnace is missing, which is not required for the synthesis of ZnSe. Chemicals were purchased from a well-known seller and chemical details are given in **table 2.2.**

Table 2.2: Details of chemicals used

Sr. No.	Chemical Name	Chemical Formula	Molar Mass (g/mol)	% Purity	Supplier
1	Zinc Powder	Zn	65.38	97	BDH
2	Selenium Powder	Se	78.96	99	Merck
3	Potassium Hydroxide	KOH	56.10	99	Sigma

First of all 35 mL solution of 3 M KOH is made in distilled water, then Zn powder (0.65 g) and Se powder (0.394 g) were added, and solution is stirred by the help of magnetic stirrer for 1 hour. Synthesized solutions is shifted to an autoclave with capacity of 40 mL and then close the autoclave tightly, later on it was putted into a simple heating oven at temperature of 120 °C. After 2 hours autoclave was moved out from oven and placed at room temperate for several hours, in this way it was cooled, naturally. Greenish precipitates were observed which were washed with distilled water and ethanol, dried and ground. Dark green product was obtained at the end.

2.3 Hydrothermal Synthesis of CoTe

0.19 g of $CoCl_2.6H_2O$ and 0.10 g of Te powder were added in 8 mL, 6 M solution of KOH. This solution is continuously stirred and 2 mL of hydrazine hydrate is also added [86]. This solution is transferred to autoclave. Autoclave was tightly packed and transfer to an oven, the temperature of oven was set to 170 °C and time was set to 24 h. The autoclave was cooled at room temperature after removing out from oven. After washing (with ethanol and distilled water), drying and grinding, product is obtained as a black powder.

Table 2.3: Chemical details for the synthesis of CoTe

Sr. No.	Chemical Name	Chemical Formula	Molecular Mass (g/mol)	% Purity	Supplier
1	Cobalt-Chloride Hexahydrate	$CoCl_2.6H_2O$	237.93	98	Panreac
2	Tellurium Powder	Te	127.6	98	Merck
3	Potassium Hydroxide	KOH	56.10	99	Sigma
4	Hydrazine Hydrate	N_2H_4	32.04	98	Uni-Chem

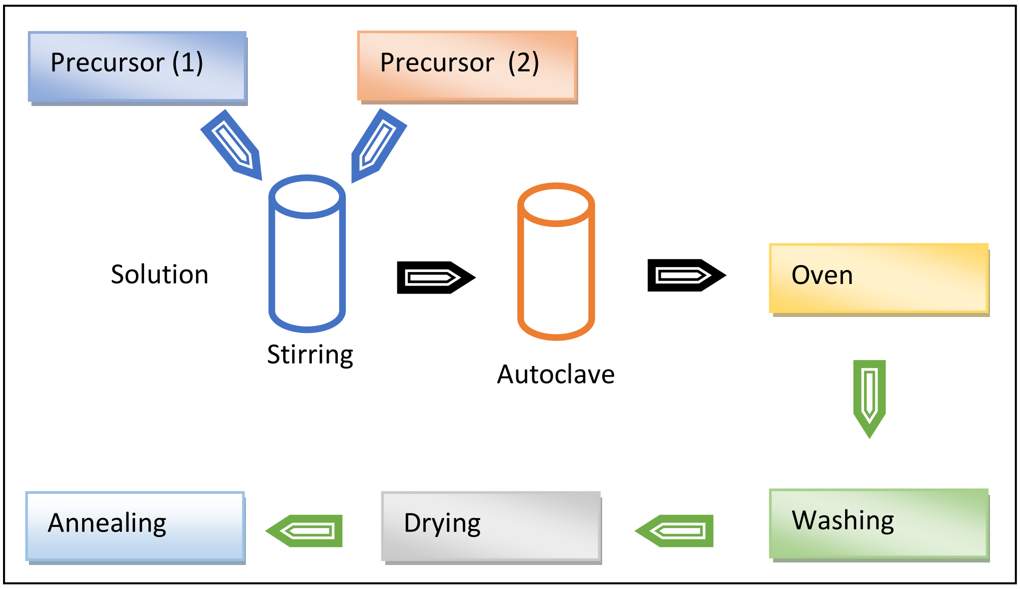

Figure 2.2. General flow sheet diagram for the hydrothermal synthesis of nanoparticles

2.4 Synthesis of Different Composites of Co_3O_4/ZnSe and Co_3O_4/CoTe

Composites with different percentages are made up by a physical method, in which different ratios of Co_3O_4, ZnSe and CoTe are ground in mortar and pestle, physically as shown in **figure 2.3.** Details of composites are given in **table 2.3** and **table 2.4.**

Figure 2.3. Mortar and Pestle

Table 2.3: Detail of Co_3O_4/ ZnSe nanocomposites

Sr. No.	**Composite Name**	**% of Co_3O_4 by Weight**	**% of ZnSe by Weight**
1	Z1	75	25
2	Z2	50	50
3	Z3	25	75

Table 2.4: Detail of Co_3O_4/ CoTe nanocomposites

Sr. No.	**Composite Name**	**% of Co_3O_4 by weight**	**% of CoTe by weight**
1	A1	75	25
2	A2	50	50
3	A3	25	75

Chapter 3: Co_3O_4/CoTe Common-Cation Nanocomposite

This chapter includes the results and discussion portion of synthesized Co_3O_4, CoTe and their composites *i.e.* Co_3O_4/CoTe. Results of photocatalytic activity are also explained here.

3.1 Crystallographic Analysis

X-ray powder diffraction (XRPD) is used for the confirmation of phase and crystal structures of synthesized Co_3O_4, CoTe, and Co_3O_4/CoTe nanocomposite as shown in **figure 3.1**. Obtained results match well with reported literature, previously. All the diffraction peaks of the synthesized Co_3O_4 confirm that nanomaterial with cubic geometry is synthesized (JCPDS: 42-1467) [89]. While the diffraction peaks of CoTe confirms the formation of single phase, hexagonal nanostructures (JCPDS: 65-8986) [90]. In case of nanocomposites of Co_3O_4 and CoTe, diffraction peaks of both the materials are present which confirms the formation of nanocomposites. Crystallite sizes were calculated by Scherrer formula, which are 20.32 nm for Co_3O_4 and 15.69 nm for CoTe.

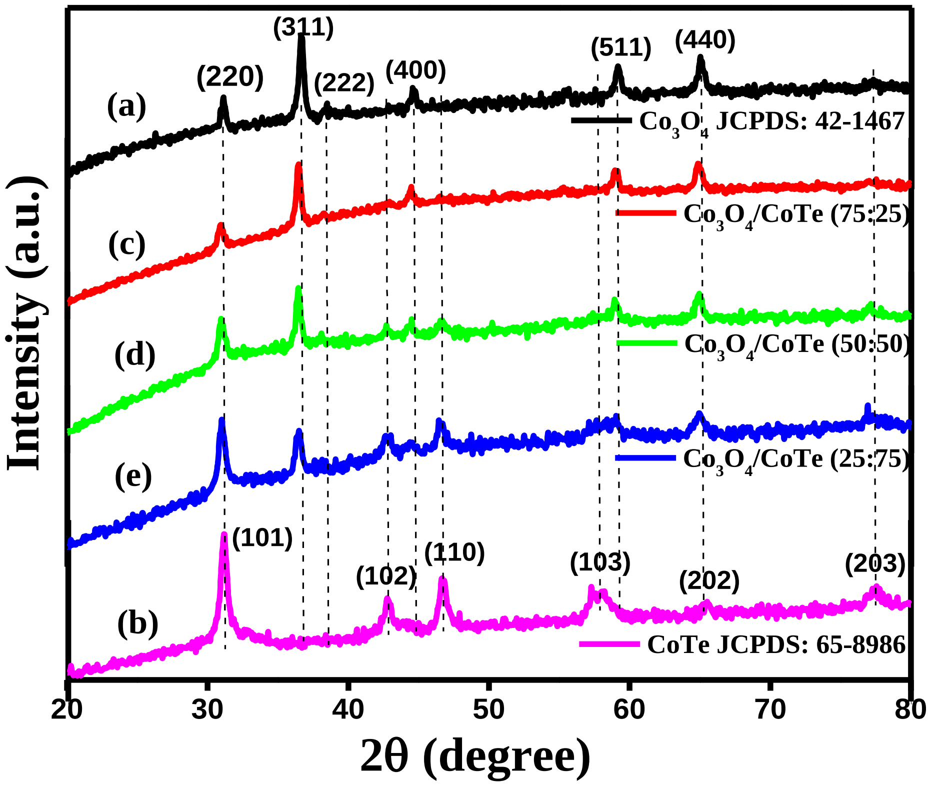

Figure 3.1. XRD patterns of (a) Co_3O_4, (b) CoTe, (c) Co_3O_4/CoTe (3:1), (d) Co_3O_4/CoTe (1:1) and (e) Co_3O_4/CoTe (1:3)

3.2 Morphological Analysis

Morphology of the synthesized nanomaterials *i.e.* bare Co_3O_4, CoTe and their nanocomposites (Co_3O_4/CoTe) was investigated by scanning electron microscopy (SEM).

From the SEM results of Co_3O_4, it was observed that, Co_3O_4 possess grain like morphology as shown in **figure 3.2 (a)**, with size approximately 20 nm. In case of CoTe nano-sheets were appeared. The thickness of nano-sheets is very small and ranges up to 15 nm. At some points in SEM image sheets of CoTe combine to form a superstructure as shown in **figure 3.2 (b).**

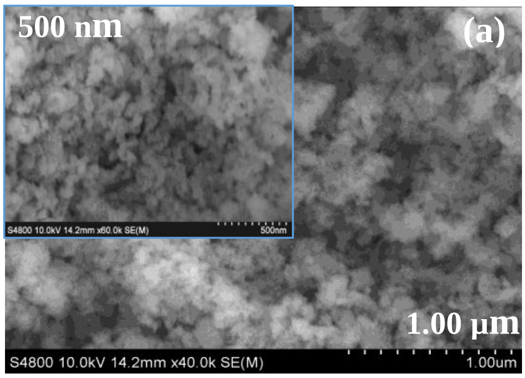

Figure 3.2. SEM images of (a) Co_3O_4 and (b) CoTe

- Three nanocomposites of CoTe with Co_3O_4 are synthesized named as A1, A2 and A3 (3:1, 1:1 and 1:3), which were also discussed in chapter # 2: table 2.5.

SEM images of all the composites are given below in **figure 3.3**, it was observed that both the materials are present *i.e.* worm like Co_3O_4 and disk like CoTe.

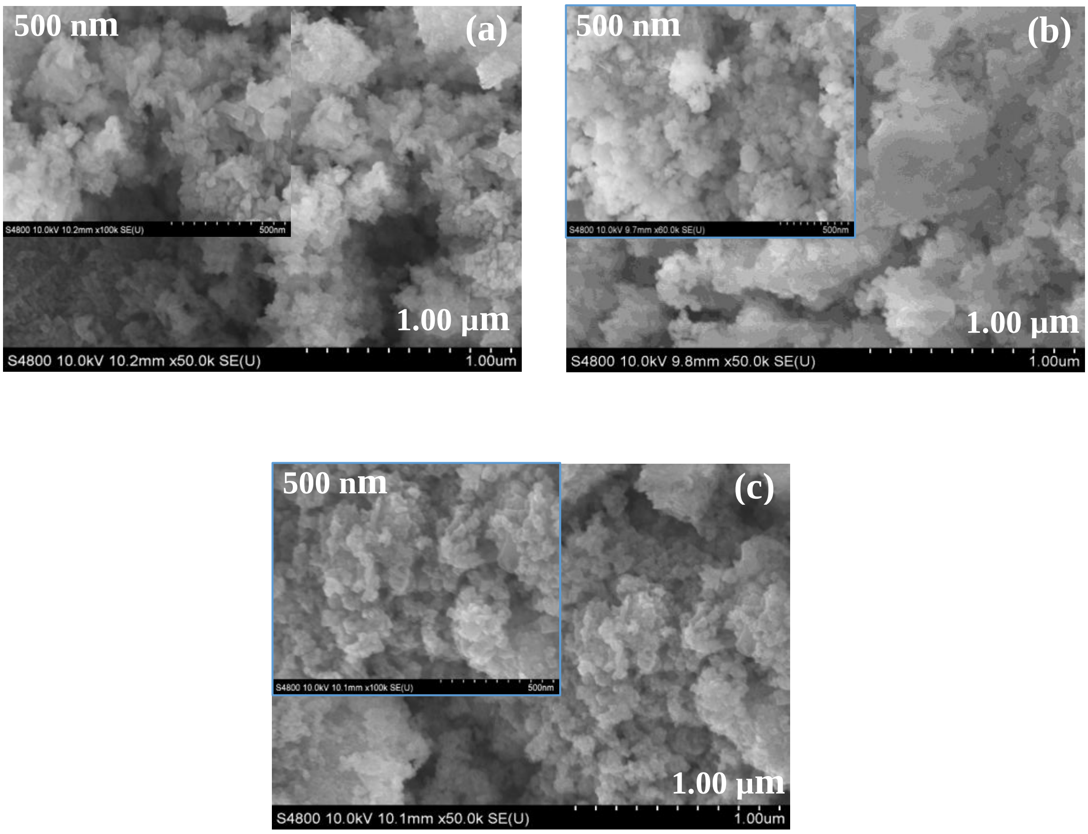

Figure. 3.3. SEM images of Co_3O_4/CoTe nanocomposites (a) A1, (b) A2 and (c) A3

3.3 Elemental Analysis

Energy dispersive X-ray spectroscopy (EDX) was used to examine elemental analysis of Co_3O_4, CoTe and their nanocomposites.

In Co_3O_4 EDX analysis confirms the presence of Cobalt (Co) and Oxygen (O) as shown in **figure 3.4 (a)**. Carbon (C) is also present in the EDX spectra, which is considered as impurity and its amount is very low. With the help of EDX percentage composition of different elements is also calculated shown in **table 3.1**. EDX Spectra is also shown **figure 3.4 (b)**, it was observed that Co and Te are present as main elements and their atomic % are also given in **table 3.2.** Carbon and oxygen are present as impurities and their atomic % is very low.

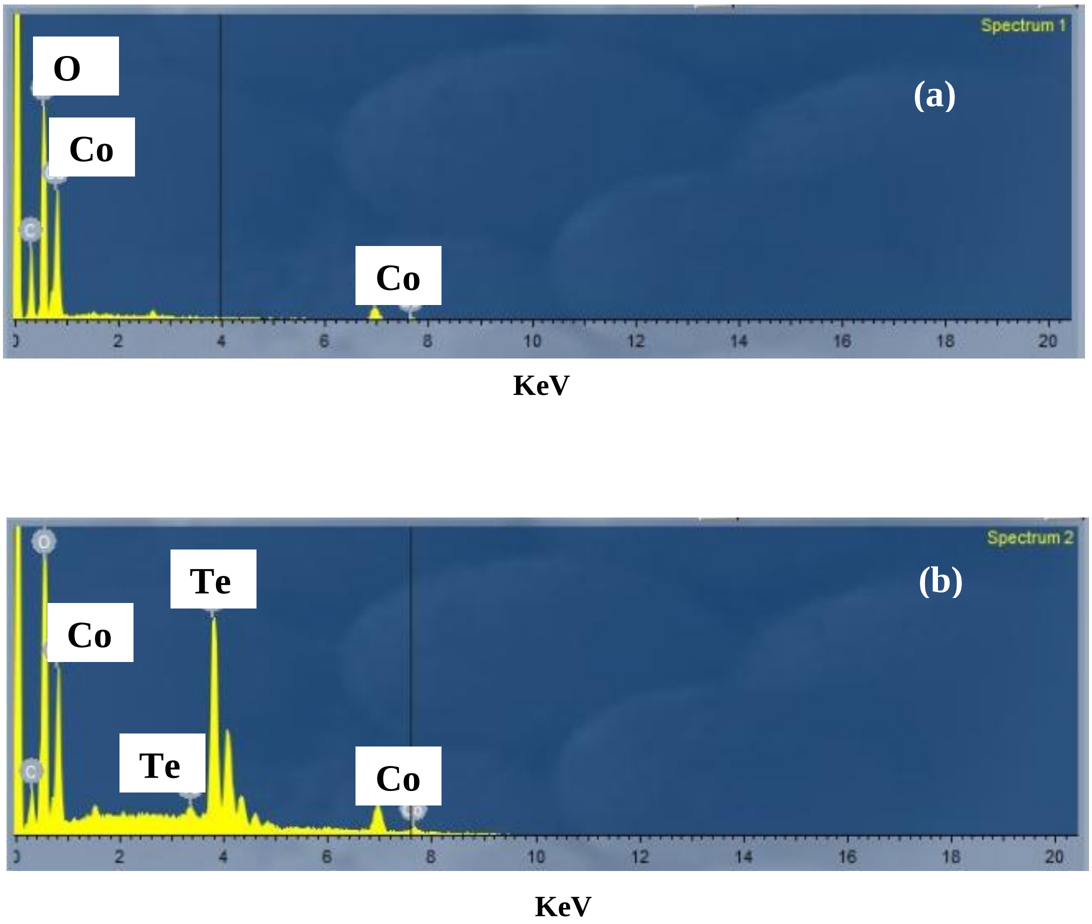

Figure 3.4. EDX analysis of Co_3O_4 (a) and CoTe (b)

Table 3.1: Elemental Composition of Co_3O_4

Element	**Weight %**	**Atomic %**
C	17.02	34.46
O	28.28	42.98
Co	54.70	22.57

Table 3.2: Elemental composition of CoTe

Element	**Weight %**	**Atomic %**
C	2.28	11.09
O	9.49	34.68
Co	25.83	25.63
Te	62.41	28.60

EDX results also confirm the formation of nanocomposites i.e. A1, A2 and A3, both the nanomaterials i.e. Co_3O_4 and CoTe are present in nanocomposites **figure 3.5 (a-c)**. Atomic and weight percentages of synthesized nanocomposites are also given in **table 3.3-3.5**. Some impurities like Cl and C are present in EDX results but their concentration is very low.

It was observed that percentage of Te is increased in A2 as compared to A1 which confirms that ratio of CoTe is increased in A2 as shown in **table 3.4**, while in A3 percentage of Te is increased more but percentage of Co is decreased as compared to A1 and A2 nanocomposites, which confirms that amount of CoTe is increased in composite A3.

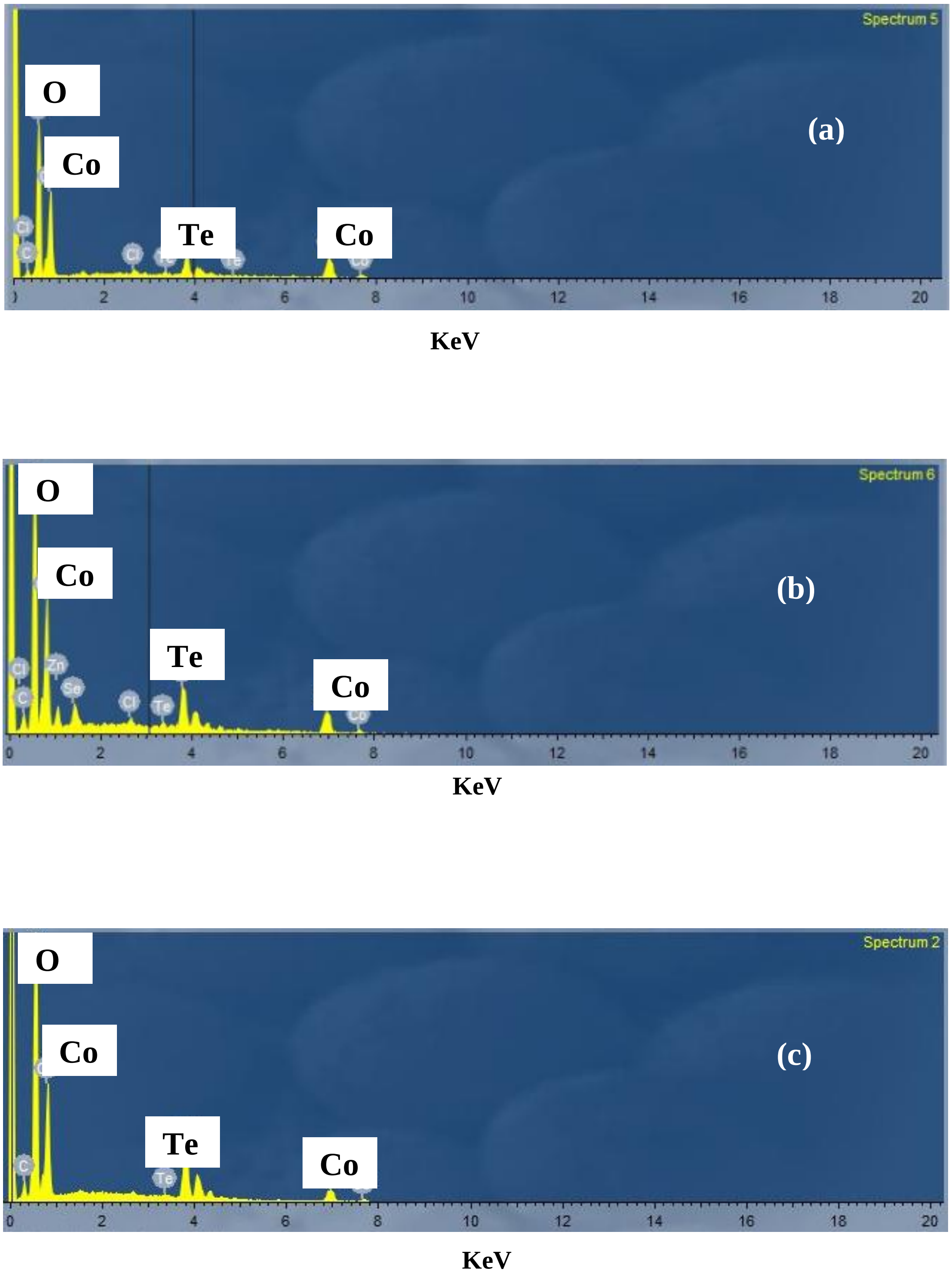

Figure 3.5. EDX analysis of Co_3O_4/CoTe nanocomposites (a) A1, (b) A2 and (c) A3

Table 3.3: Elemental composition of A1

Element	**Weight %**	**Atomic %**
C	2.93	9.09
O	21.55	50.21
Cl	1.36	1.43
Co	51.73	32.72
Te	22.43	6.55

Table 3.3: Elemental composition of A2

Element	**Weight %**	**Atomic %**
C	3.17	10.61
O	18.63	46.83
Cl	1.00	1.14
Co	42.18	28.78
Zn	3.59	2.21
Se	2.74	1.39
Te	28.69	9.04

Table 3.3: Elemental composition of A3

Element	**Weight %**	**Atomic %**
C	2.73	9.34
O	19.55	50.16
Co	41.39	28.82
Te	36.33	11.69

3.4 Optical Properties and Bandgap Estimation

UV-Visible spectroscopy is used to determine optical properties and bandgaps of Co_3O_4 and CoTe are measured. In semiconductor nanomaterials quantum confinement effect can be observed. If the dimensions of semiconductor are smaller as compared to the Bohr radius of excited state, absorption is shifted to higher energy [91, 92]. The optical band gap of a semiconductor also depends upon the crystallite size, crystallite size is inversely related to band gap [92]. These both effects are observed during calculating the bandgap, because bandgap is little higher as compared to usually observed value.

In UV-visible spectra of Co_3O_4 there are two prominent peaks as shown in **figure 3.6 (a)**. One peak is at 510 nm and second is at 684 nm. We can calculate the bandgap of semiconductor nanomaterial from UV-visible data by using following equation [93],

$$(\alpha h\nu)^n = B(h\nu\text{-}Eg) \ \ldots\ldots\ (3.1)$$

where,

$h\nu$ = Photon energy (eV)

A = Absorption coefficient

B = Constant relative to material

Eg = Band gap

n = ½ for an indirect transition and 2 for direct transition

The optical band gap of Co_3O_4 is measured by Tauc plot, which is a curve between $(\alpha h\nu)^2$ on Y-axis and $h\nu$(eV) on X-axis. Optical bandgap energy is calculated by extrapolating the graph. Co_3O_4 possess two bandgaps, generally appear in the range of 1.5 to 2.5 [94-97]. Here in this work, two bandgaps of Co_3O_4 are also appeared **figure 3.6 (b) and 3.6 (c)**, one is located at 2.51 eV which is observed due to O^{2-} to Co^{2+} charge transfer (fundamental band gap or valance to conduction band excitation), and other is located at 2.2 eV which is observed due to O^{2-} to Co^{3+} charge transfer (Co^{3+} level is located below the conduction band). In the Tauc plot UV-Visible absorption is divided into two parts *i.e.* from 400 nm- 515 nm and 500 nm-800 nm, both the band gaps of Co_3O_4 are shown separately as shown by some other researchers [98, 99].

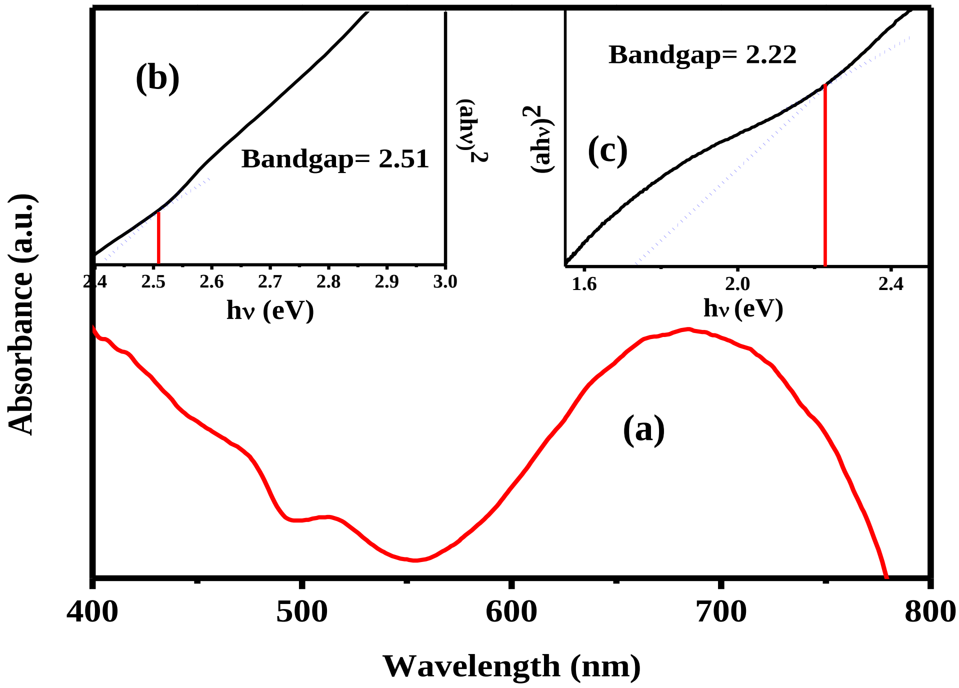

Figure 3.6. (a) UV-Vis Spectrum (b, c) Tauc plots of Co_3O_4

In case of CoTe UV-visible spectra exhibits two peaks, one peak is present at 473 nm, while other peak is observed at 518 nm. Due to extreme anisotropy of band structure and band mixing, peaks are broad [86]. Tauc plot is made to calculate the bandgap of CoTe and it was observed that it has bandgap of 2.24 eV, which matches well with the previously reported value [86]. UV-visible spectra and bandgap of CoTe is shown in **figure 3.7**.

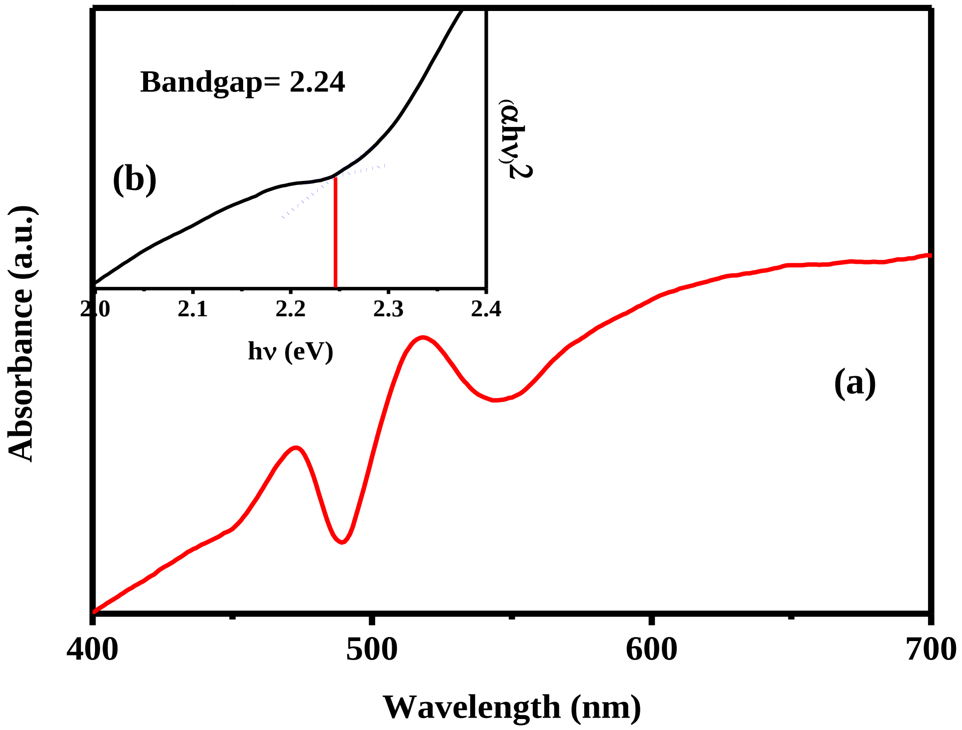

Figure 3.7. (a) UV-Vis spectrum and (b) Tauc plot of CoTe

It is reported in literature that XPS technique is used to calculate the valance band edge of synthesized nanomaterials [86]. Position of conduction band can be calculated by using following formula, where Ec is conduction band energy, Ev is valance band energy and Bg is calculated bandgap of the material.

$$Ec = Ev - Bg\text{………} \quad (3.2)$$

Bandgap alignment, position of conduction band and valance band edge of synthesized Co_3O_4/CoTe nanocomposite is given in **figure 3.8**, which indicates that it can be used for photocatalytic applications under UV-Visible light.

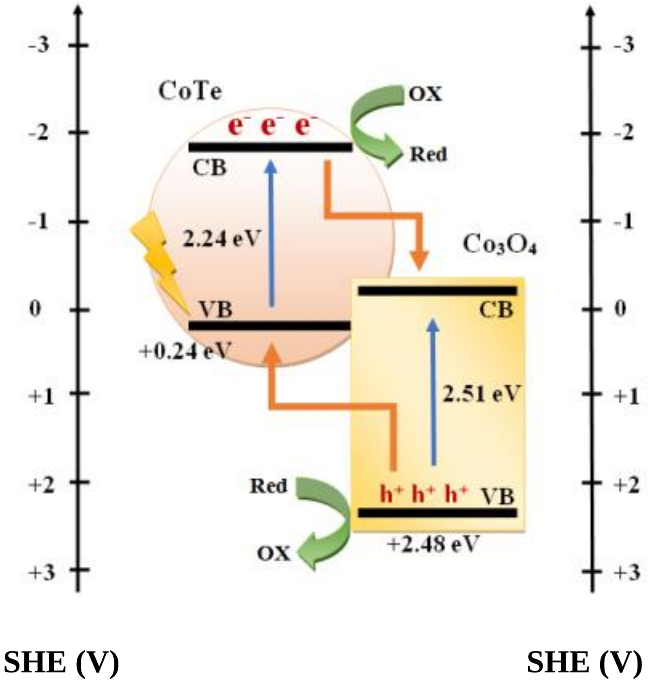

Figure 3.8. Bandgap alignment of Co_3O_4/CoTe

3.5 Photocatalytic Activity of Co_3O_4/CoTe

Synthesized nanomaterials *i.e.* Co_3O_4, CoTe and their nanocomposites (Co_3O_4/CoTe) are used for the degradation of organic dye: Congo red. UV-Visible spectrophotometer is used to calculate the λmax value of dye. 300 W Xe arc lamp was used as light source and it was placed at a distance of 15 cm higher, over the vessel which contains the solution of Congo red dye and photocatalyst.

In the absence of light a solution of 100 mg of photocatalyst and 100 mg of Congo red was made. After the continuous stirring of 10 min the solution is placed under UV-Visible light and after each 5 min time interval; 5 mL solution was taken out to check the percentage degradation.

Series of experiments are performed to check the dye degradation ability of pristine nanomaterials and their nanocomposites. Blank experiment was also performed and it was confirmed that dye cannot be degraded without photocatalyst or without light.

It was observed that degradation rate of pristine Co_3o_4, CoTe nanomaterials is very low under UV-Visible irradiation. Enhanced photocatalytic activity has been observed when Co_3O_4/CoTe nanocomposite is used.

When UV-Visible light is irradiated on the solution of Congo red dye and Co_3O_4/CoTe nanocomposite; dye degradation starts and dye is degraded gradually. After the 60 min of light irradiation, degradation reaches up to 96 %, but in case of pure Co_3O_4 or CoTe % degradation is very low which is just 20 % and 15 % respectively, as shown in **figure 3.9.**

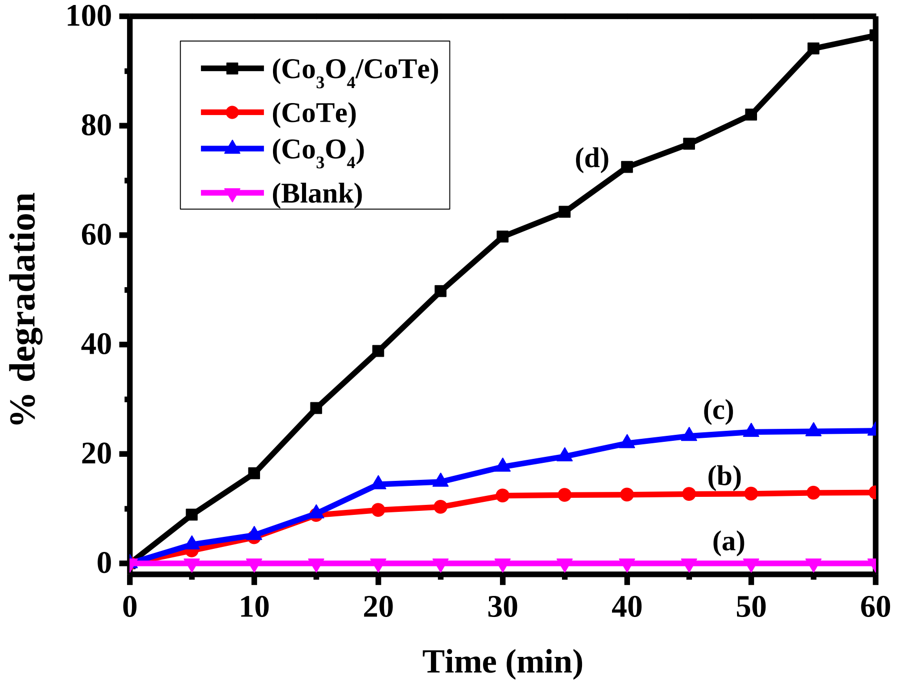

Figure 3.9. Dye degradation by (a) blank (b) CoTe (c) Co_3O_4 and (d) Co_3O_4/CoTe

3.6 Mechanism of Photocatalysis

When light is irradiated on a photocatalytic system; electron-hole pair is generated. Electrons move to the conduction band while holes left behind in valance band of the photocatalyst. This electron-hole pair acts as a base for photocatalysis because they take part in redox reaction. But there are chances of electron-hole recombination which can cease the photocatalytic activity; there are different methods to overcome the electron-hole recombination, as discussed earlier. Here nanocomposites are made to prevent from recombination of charges as shown in **figure 3.8.**

Nanocomposites *i.e.* Co_3O_4/CoTe have shown high photocatalytic activity because their band structure and bandgap alignment become very suitable for photocatalytic activity and electron-hole recombination is reduced. In the nanocomposite electrons of CoTe migrate to the conduction band of Co_3O_4 while holes of Co_3O_4 migrate to the valance band of CoTe. In this way the electron-hole recombination is reduced and rate of oxidation-reduction reaction increases, as a result photocatalytic activity also increases.

It is also noted that, in nanocomposite which contains a common cation or anion (AB/AC), an addition barrier is formed which is actually an interface with larger energy gap as compared to bandgap of the photocatalyst, and it helps in the separation of charge carrier [110]. If no common cation or anion is present in a photocatalytic system (AB/CD) then the interface with smaller energy gap as compared to band gap of the photocatalyst arises which might act as charge trap in the form of quantum well, and reduce the photocatalytic activity, as shown in **figure 3.10** [100]. This is the reason of higher photocatalytic activity of Co_3O_4/CoTe as compared to Co_3O_4/ZnSe because in Co_3O_4/CoTe common cation (Co^{2+}) is present.

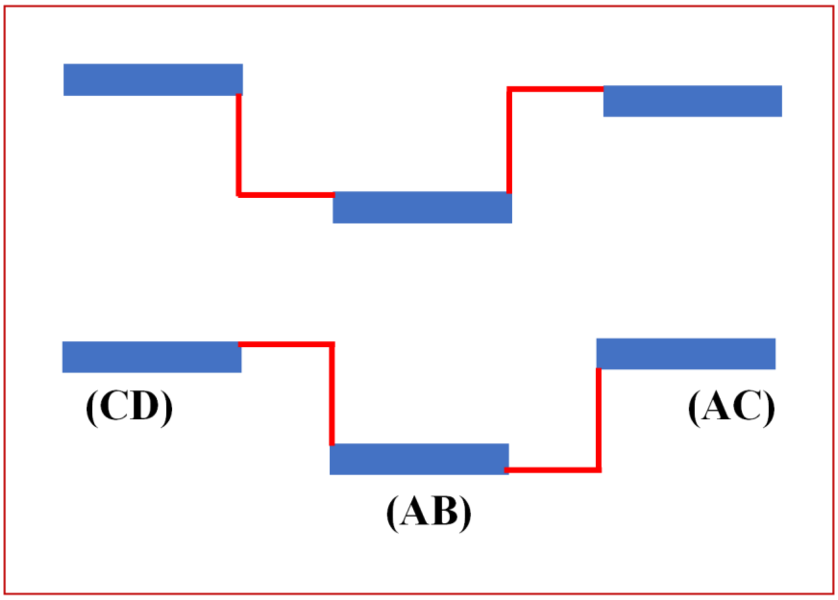

Figure 3.10. Heterostructures with and without common cation

Chapter 4: Co_3O_4/ZnSe Nanocomposite

4.1 Crystallographic Analysis

XRD results of ZnSe as shown in **figure 4.1** indicate the presence of both cubic and hexagonal structures. In XRD pattern, five peaks appear at 2θ = 27.2°, 45.1°, 53.5°, 65.9° and 72.7°. According to the JCPDS Card No: 3-065-9602 [101] these peaks indicate that product is cubic ZnSe and (111), (220), (311), (400), (331) are diffraction lines of it. Other peaks present at 2θ= 26.2°, 29.5°, 36.1° and 68.2° are indexed as (100), (101), (102), and (203) are the diffraction lines of hexagonal ZnSe (JCPDS 1-080-008).

Nanocomposite of Co_3O_4 and ZnSe contain the peaks of both the materials which confirm the formation of Co_3O_4-CoTe nanocomposite as shown in **figure 4.1**. Peaks of Co_3O_4 are shown by number sign **(#)** while peaks of ZnSe are shown by asterisk sign **(*)**. Particle size of ZnSe is 16.56 nm, calculated by Scherrer formula.

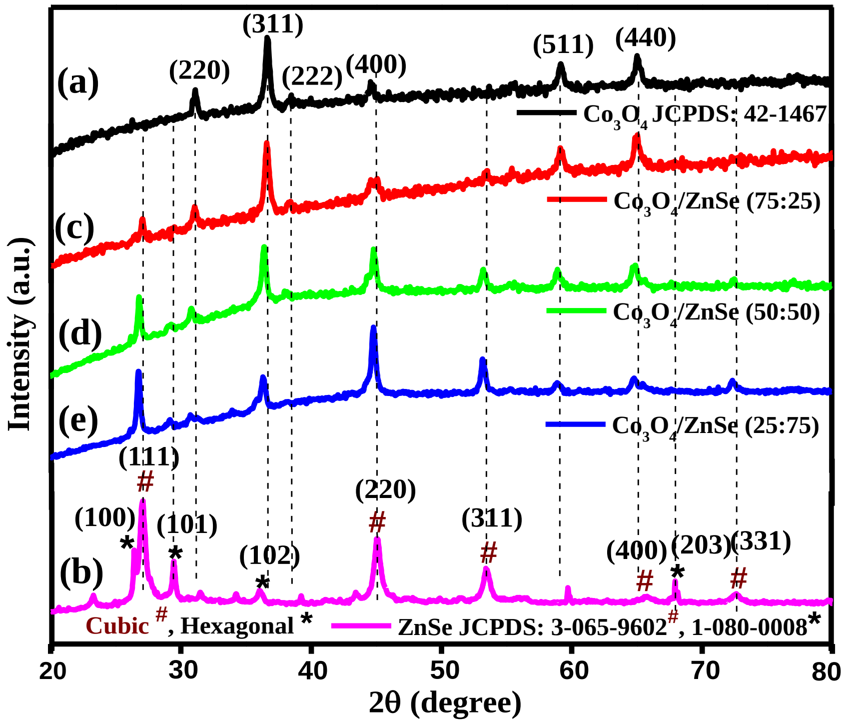

Figure 4.1. XRD pattern of (a) Co_3O_4, (b) ZnSe, (c) Co_3O_4/ZnSe (3:1), (d) Co_3O_4/ZnSe (1:1) and (e) Co_3O_4/ZnSe (1:3)

4.2 Morphological Analysis

In case of ZnSe it was observed that a mixed morphology is appeared. Some nanoparticles are spherical in shape while other are distorted cubes or grains. Size of ZnSe nanoparticles is approximately 16 nm which matches well with size calculated by Scherrer formula. ZnSe nanoparticles are present in the form of agglomerates as shown in SEM image **figure 4.2.**

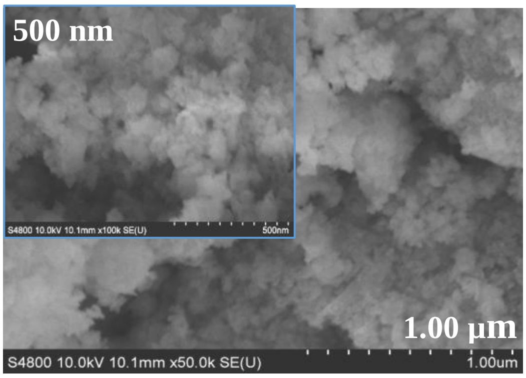

Figure 4.2. SEM images of ZnSe

- There are three nanocomposites of ZnSe with Co_3O_4 are synthesized named as Z1, Z2 and Z3 (3:1, 1:1 and 1:3); which are also discussed in chapter # 2: table 2.4.

In SEM images of composite Z1 few grain like Co_3O_4 are observed but most of the Co_3O_4 nanoparticles are covered by agglomerates of ZnSe, which has mixed morphology, as shown in **figure 4.3 (a)**.

Composite Z2 contain the Co_3O_4 and ZnSe with equal amounts by weight (1:1). In SEM image grain like Co_3O_4 are easily observed and the other nanoparticles having mixed morphology are indicating the presence of ZnSe as shown in **figure 4.3 (b)**.

SEM results of composite Z3 indicate that agglomerates of Co_3O_4 and ZnSe are formed, due to higher amount of ZnSe mixed morphology is appeared but at some points, grain like Co_3O_4 are also present as shown in **figure 4.3 (c).**

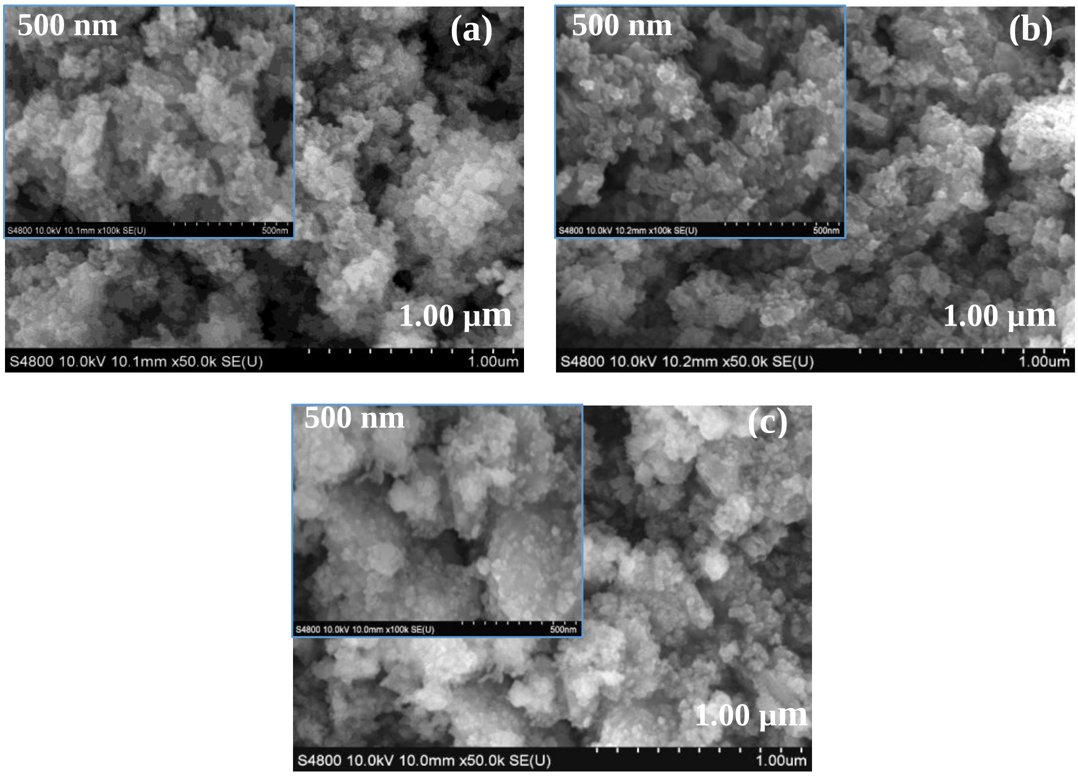

Figure 4.3. SEM images of Co_3O_4/ZnSe nanocomposites *i.e.* (a) Z1, (b) Z2 and (c) Z3

4.3 Elemental Analysis

EDX spectra and elemental composition of ZnSe are given below **figure 4.4** and **table 4.1**, which confirms the presence of Zn and Se.

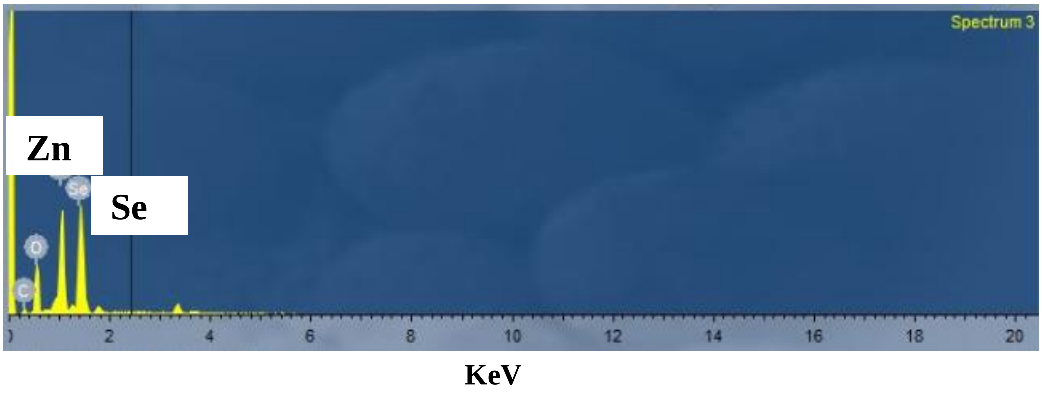

Figure 4.4. EDX analysis of ZnSe

Table 4.1: Elemental composition of ZnSe

Element	Weight %	Atomic %
C	6.29	19.35
O	18.35	42.40
Zn	30.39	17.19
Se	44.98	21.06

EDX results of nanocomposites are shown below in **figure 4.5 (a-c)**, the results confirm that the presence of Co, O, Zn and Se elements. In case of Z1 from the atomic percentages of element as shown in **table 4.2**, it is observed that atomic percentage of Zn and Se is very low as compared to Co_3O_4 which confirms that ratio of Co_3O_4 and ZnSe is 3:1.

Weight and atomic percentages of elements of sample Z2 shows that atomic percentage of Zn and Se is increased as compared to Z1, while atomic percentage of Co and O is decreased, which confirms the 1:1 concentration of Co_3O_4 and ZnSe as shown in **figure 4.5 (b)** and **table 4.3**.

In nanocomposite Z3 percentage of ZnSe is increased more, but percentage of Co_3O_4 is decreased which confirms that of ZnSe and Co_3O_4 are present in 3:1, respectively, as shown in **figure 4.5 (c)** and **table 4.4**. Few impurities like K and Si are also observed but in very minute amount.

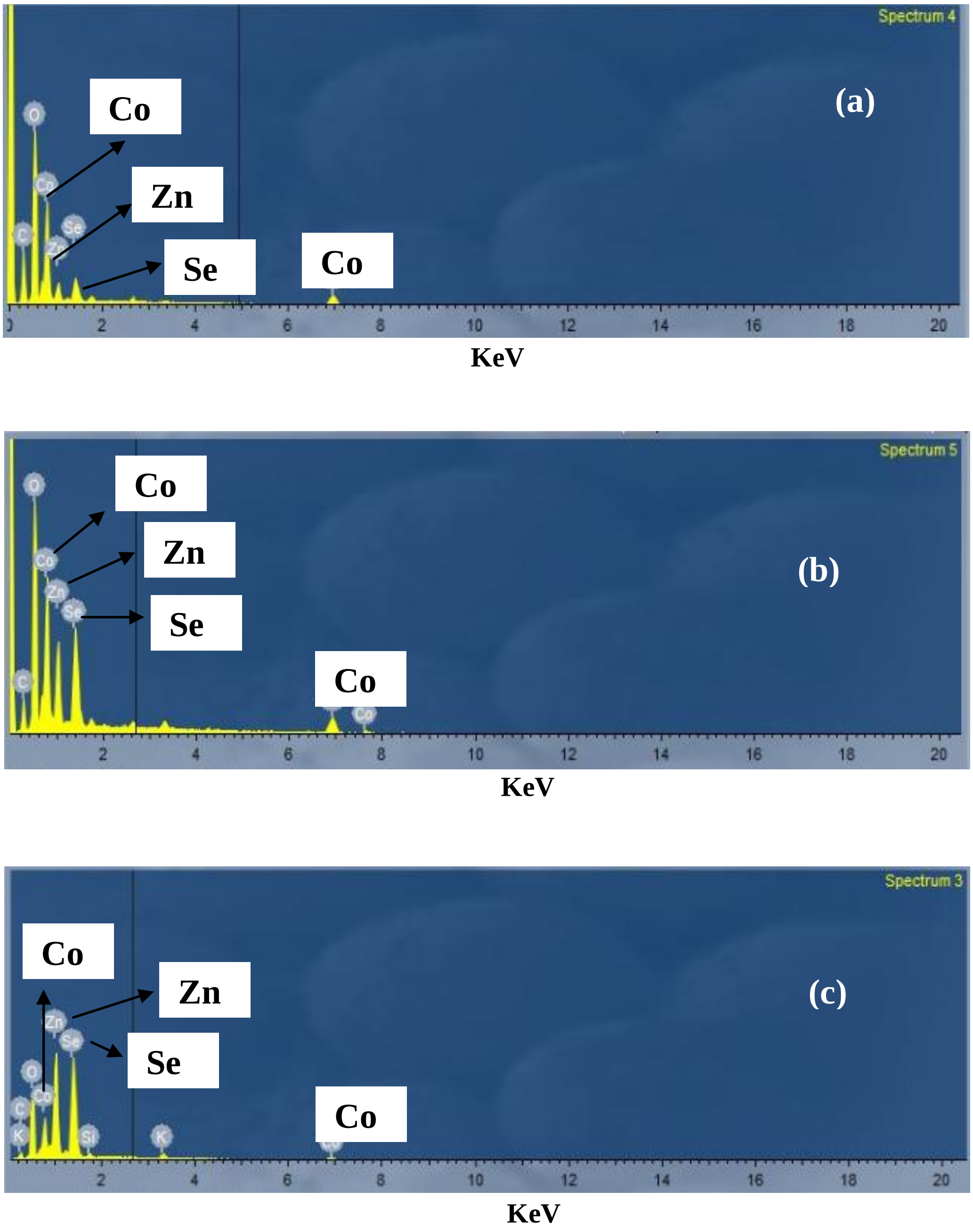

Figure 4.5. EDX analysis of composite Z1 (a), Z2 (b) and Z3 (c)

Table 4.2: Elemental composition of composite Z1

Element	Weight %	Atomic %
C	15.74	33.54
O	28.25	42.00
Co	48.25	20.96
Zn	4.99	1.95
Se	4.77	1.55

Table 4.3: Elemental composition of composite Z2

Element	Weight %	Atomic %
C	8.19	21.57
O	22.08	43.67
Co	41.38	22.22
Zn	14.09	6.82
Se	14.27	5.72

Table 4.4: Elemental composition of composite Z3

Element	Weight %	Atomic %
C	4.54	14.71
O	15.70	38.23
Si	0.78	1.08
K	1.76	1.76
Co	19.93	13.17
Zn	27.22	16.22
Se	30.07	14.83

4.3.1 **Optical Studies and Bandgap Estimation**

UV-Visible absorption spectra of ZnSe and Tauc plot are presented in **figure 4.6**, which shows that bandgap of ZnSe is 2.64 eV, which matches quite well with reported value [102]. By XPS studies from literature, valance band edge is known. Position of conduction band of ZnSe is calculated by position of valance band and value of bandgap, by using equation (3.2).

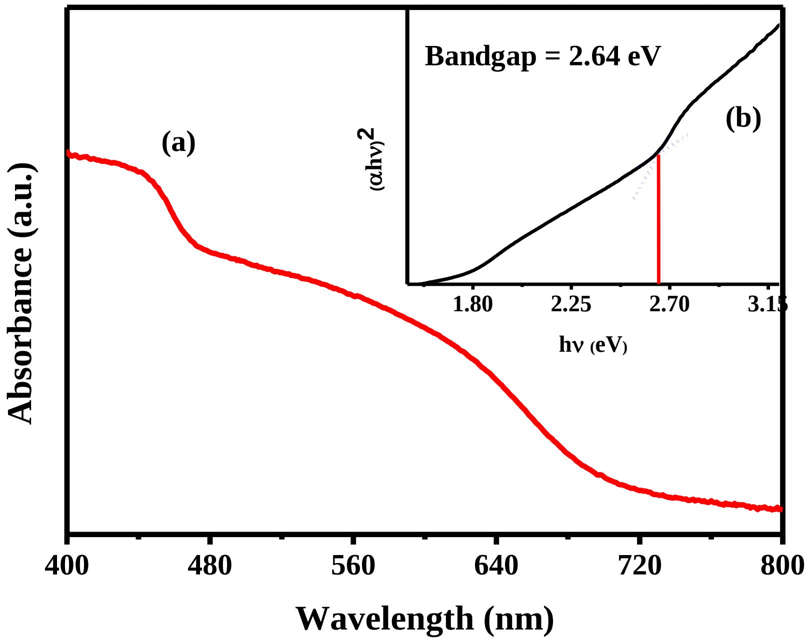

Figure 4.6. (a) UV-Vis spectrum and (b) Tauc plot of ZnSe

Bandgap alignment of Co_3O_4/ZnSe nanocomposite is shown in **figure 4.7**, which indicates that Co_3O_4/ZnSe is suitable for photocatalytic activity under UV-visible light.

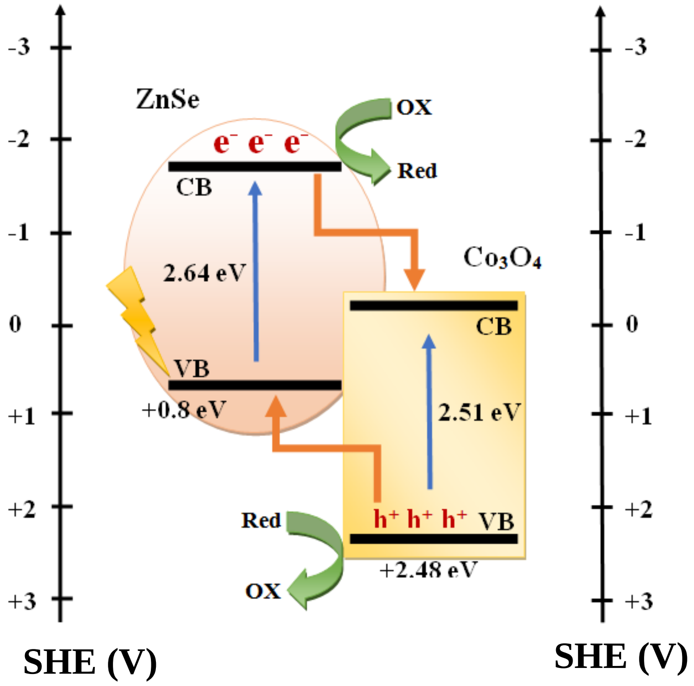

Figure 4.7. Bandgap alignment of Co_3O_4/ZnSe

4.4 Photocatalytic Activity of Co_3O_4/ZnSe

In case of Co_3O_4/ZnSe, same mechanism was used to check its photocatalytic activity, as used for the Co_3O_4/CoTe, already discussed in chapter # 3. It was expected that nanocomposite would show enhanced dye degradation ability as compared to pristine Co_3O_4. But an unexpected behavior is observed here because degradation rate of bare ZnSe is greater than the nanocomposite of Co_3O_4/ZnSe. This might be attributed to the presence of two combined phases of ZnSe here, which are cubic and hexagonal, as confirmed by XRD pattern **(Figure 4.1)**. So here, ZnSe itself acting as a composite, but the exact mechanism is still not known and we will try to find the reason in future. Photocatalytic activities of nanomaterials are shown in **figure 4.8**.

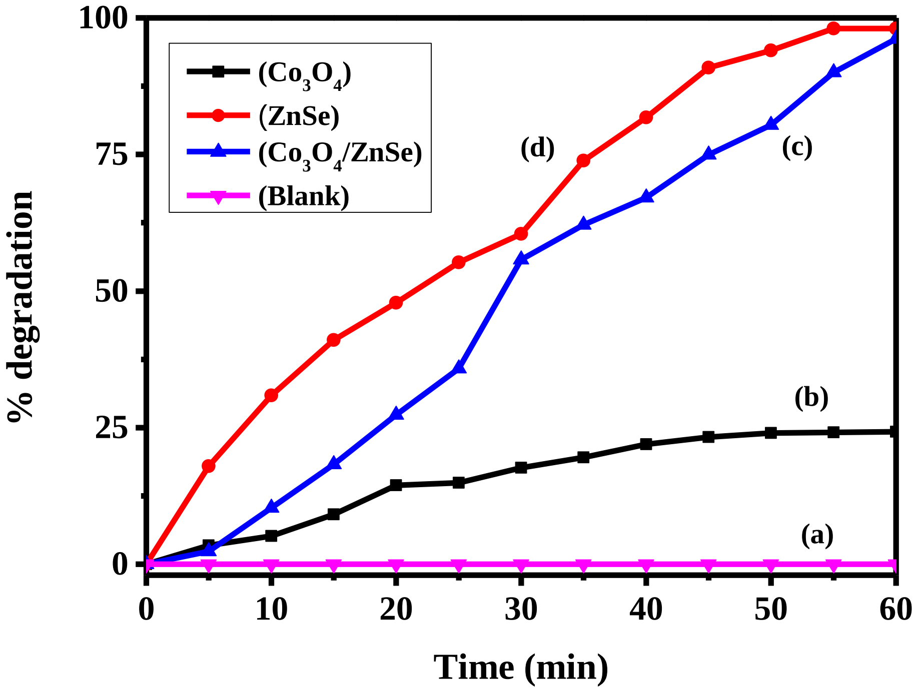

Figure 4.8. Dye degradation by (a) blank (b) Co_3O_4 (c) Co_3O_4/ZnSe (d) bare ZnSe photocatalysts

4.5 Conclusion

Semiconductor nanomaterials and their nanocomposites are made successfully. It was observed that particle sizes of the produced nanomaterials are very small which works well for photocatalytic application. Bandgaps of synthesized nanomaterials are very suitable for photocatalytic activity because in case of nanocomposites charges are separated well and charge recombination is reduced; as a result photocatalytic activity is increased which was confirmed by degrading organic dye.

Chapter 5: Conclusion and Future Prospects

This chapter includes the conclusion of the research work performed and also it discusses the future prospects of this work.

5.1 Conclusion

- In the present work synthesis of nanoparticles and their photocatalytic properties and applications are described.
- Brief literature survey is done to find out nanomaterial; having suitable bandgap for photocatalysis; Co_3O_4, CoTe and ZnSe are found as suitable semiconductors.
- It was found by the literature that photocatalytic activity of semiconductor photocatalysts can be improved by different method, and one of the best method; is production of nano heterostructures or nanocomposites.
- A simple hydrothermal method is used to synthesize nanomaterials.
- Different composites of nano materials *i.e.* Co_3O_4/CoTe and Co_3O_4/ZnSe are made by simple physical method.
- Characterization of the synthesized nanomaterials is performed by different techniques; like XRD, SEM, EDX and UV-Visible spectroscopy which confirms that nanomaterials are synthesized successfully.
- To check the photocatalytic activity; synthesized nanomaterials were used for the degradation of Congo red dye.
- It was found that Co_3O_4/CoTe nanocomposites have enhanced photocatalytic activity as compared to pristine nanomaterials.
- The photocatalytic activity of bare ZnSe in higher as compared to its composite *i.e.* Co_3O_4/ZnSe. It was attributed to the mixed phase of ZnSe, which may be itself acting as nanocomposite. But the exact reason is not known and we shall try to find it out in future.

5.2 Future Prospects

- Study of photocatalytic activity of bare ZnSe.
- Use of different methods; like doping and formation of co-catalysts to enhance the photocatalytic activity and absorption range of synthesized nanomaterial.
- To find out the other photocatalytic applications of synthesized nanomaterials like CO_2 reduction and H_2 production.

References

References

[1] L.-B. Li, J.-L. Hu, and N.-C. Xia, "Industrial energy-pollution performance of regions in China based on a unified framework combining static and dynamic indexes," *Journal of Cleaner Production,* vol. 131, pp. 341-350, 2016.

[2] J. Cheng, S. Dai, and X. Ye, "Spatiotemporal heterogeneity of industrial pollution in China," *China Economic Review,* vol. 40, pp. 179-191, 2016.

[3] A. Haines, R. S. Kovats, D. Campbell-Lendrum, and C. Corvalán, "Climate change and human health: impacts, vulnerability and public health," *Public health,* vol. 120, pp. 585-596, 2006.

[4] Y. Zheng, Z. Li, S. Feng, M. Lucas, G. Wu, Y. Li, *et al.*, "Biomass energy utilization in rural areas may contribute to alleviating energy crisis and global warming: A case study in a typical agro-village of Shandong, China," *Renewable and Sustainable Energy Reviews,* vol. 14, pp. 3132-3139, 2010.

[5] K. Lo, "A critical review of China's rapidly developing renewable energy and energy efficiency policies," *Renewable and Sustainable Energy Reviews,* vol. 29, pp. 508-516, 2014.

[6] J. Liu and J. Diamond, "China's environment in a globalizing world," *Nature,* vol. 435, pp. 1179-1186, 2005.

[7] S. Mekhilef, R. Saidur, and A. Safari, "A review on solar energy use in industries," *Renewable and Sustainable Energy Reviews,* vol. 15, pp. 1777-1790, 2011.

[8] G. He, M. Fan, and M. Zhou, "The effect of air pollution on mortality in China: Evidence from the 2008 Beijing Olympic Games," *Journal of Environmental Economics and Management,* vol. 79, pp. 18-39, 2016.

[9] O. Raaschou-Nielsen, Z. J. Andersen, R. Beelen, E. Samoli, M. Stafoggia and G. Weinmayr, "Air pollution and lung cancer incidence in 17 European cohorts: prospective analyses from the European Study of Cohorts for Air Pollution Effects (ESCAPE)," *The lancet oncology,* vol. 14, pp. 813-822, 2013.

[10] J. Tollefson, "How green is my future? UN panel foresees big growth in renewable energy, but policies will dictate just how big," *Nature,* vol. 473, pp. 134-136, 2011.

References

[11] D. S. Mathew and R.-S. Juang, "An overview of the structure and magnetism of spinel ferrite nanoparticles and their synthesis in microemulsions," *Chemical Engineering Journal,* vol. 129, pp. 51-65, 2007.

[12] P. BUSECK, S. TSIPURSKY, and R. Hettich, "Fullerenes from the geological environment," *Science,* vol. 257, pp. 215-217, 1992.

[13] C. Dekker, "Carbon nanotubes as molecular quantum wires," *Physics today,* vol. 52, pp. 22-30, 1999.

[14] B. Uyusur, C. J. Darnault, P. T. Snee, E. Kokën, A. R. Jacobson, and R. R. Wells, "Coupled effects of solution chemistry and hydrodynamics on the mobility and transport of quantum dot nanomaterials in the vadose zone," *Journal of contaminant hydrology,* vol. 118, pp. 184-198, 2010.

[15] J. R. McElhanon and D. V. McGrath, "Toward chiral polyhydroxylated dendrimers. Preparation and chiroptical properties," *The Journal of organic chemistry,* vol. 65, pp. 3525-3529, 2000.

[16] S. Zhang, D. Sun, Y. Fu, and H. Du, "Recent advances of superhard nanocomposite coatings: a review," *Surface and Coatings Technology,* vol. 167, pp. 113-119, 2003.

[17] T. P. Yadav, R. M. Yadav, and D. P. Singh, "Mechanical milling: a top down approach for the synthesis of nanomaterials and nanocomposites," *Nanoscience and Nanotechnology,* vol. 2, pp. 22-48, 2012.

[18] C. Burda, X. Chen, R. Narayanan, and M. A. El-Sayed, "Chemistry and properties of nanocrystals of different shapes," *Chemical reviews,* vol. 105, pp. 1025-1102, 2005.

[19] O. Carp, C. L. Huisman, and A. Reller, "Photoinduced reactivity of titanium dioxide," *Progress in solid state chemistry,* vol. 32, pp. 33-177, 2004.

[20] K. Nagaveni, G. Sivalingam, M. Hegde, and G. Madras, "Solar photocatalytic degradation of dyes: high activity of combustion synthesized nano TiO_2," *Applied Catalysis B: Environmental,* vol. 48, pp. 83-93, 2004.

[21] K. Nagaveni, M. Hegde, N. Ravishankar, G. Subbanna, and G. Madras, "Synthesis and structure of nanocrystalline TiO_2 with lower band gap showing high photocatalytic activity," *Langmuir,* vol. 20, pp. 2900-2907, 2004.

[22] K. S. Suslick and D. J. Flannigan, "Inside a collapsing bubble: sonoluminescence and the conditions during cavitation," *Annu. Rev. Phys. Chem.,* vol. 59, pp. 659-683, 2008.

References

[23] K. S. Suslick, "Sonochemistry," *science,* vol. 247, pp. 1439-1446, 1990.

[24] R. A. Laudise, *The growth of single crystals*: Prentice Hall, 1970.

[25] K. Byrappa and M. Yoshimura, "Handbook of Hydrothermal Technology A technology for Crystal Growth and Materials Processing," *Toronto, William Andrew Publishing,* pp. 531-535, 2001.

[26] E. Roduner, "Size matters: why nanomaterials are different," *Chemical Society Reviews,* vol. 35, pp. 583-592, 2006.

[27] B. O. Dabbousi, J. Rodriguez-Viejo, F. V. Mikulec, J. R. Heine, H. Mattoussi, R. Ober, *et al.*, "(CdSe) ZnS core− shell quantum dots: synthesis and characterization of a size series of highly luminescent nanocrystallites," *The Journal of Physical Chemistry B,* vol. 101, pp. 9463-9475, 1997.

[28] Q. H. Wang, K. Kalantar-Zadeh, A. Kis, J. N. Coleman, and M. S. Strano, "Electronics and optoelectronics of two-dimensional transition metal dichalcogenides," *Nature nanotechnology,* vol. 7, pp. 699-712, 2012.

[29] A. Hamnett, "Mechanism and electrocatalysis in the direct methanol fuel cell," *Catalysis Today,* vol. 38, pp. 445-457, 1997.

[30] W. Kreuter and H. Hofmann, "Electrolysis: the important energy transformer in a world of sustainable energy," *International Journal of Hydrogen Energy,* vol. 23, pp. 661-666, 1998.

[31] I. Fujishima and K. Honda, "Photoelectrolysis of water using titanium oxide," *Nature,* vol. 238, p. 38, 1972.

[32] A. J. Nozik, M. C. Beard, J. M. Luther, M. Law, R. J. Ellingson, and J. C. Johnson, "Semiconductor quantum dots and quantum dot arrays and applications of multiple exciton generation to third-generation photovoltaic solar cells," *Chemical reviews,* vol. 110, pp. 6873-6890, 2010.

[33] D. V. Talapin, J.-S. Lee, M. V. Kovalenko, and E. V. Shevchenko, "Prospects of colloidal nanocrystals for electronic and optoelectronic applications," *Chem. Rev,* vol. 110, pp. 389-458, 2010.

[34] I. Gur, N. A. Fromer, M. L. Geier, and A. P. Alivisatos, "Air-stable all-inorganic nanocrystal solar cells processed from solution," *Science,* vol. 310, pp. 462-465, 2005.

[35] P. V. Kamat, K. Tvrdy, D. R. Baker, and J. G. Radich, "Beyond photovoltaics: semiconductor nanoarchitectures for liquid-junction solar cells," *Chemical reviews,* vol. 110, pp. 6664-6688, 2010.

References

[36] A. Kudo and Y. Miseki, "Heterogeneous photocatalyst materials for water splitting," *Chemical Society Reviews,* vol. 38, pp. 253-278, 2009.

[37] M. V. Dozzi and E. Selli, "Doping TiO_2 with p-block elements: effects on photocatalytic activity," *Journal of Photochemistry and Photobiology C: Photochemistry Reviews,* vol. 14, pp. 13-28, 2013.

[38] X. Li, Z. Zhuang, W. Li, and H. Pan, "Photocatalytic reduction of CO_2 over noble metal-loaded and nitrogen-doped mesoporous TiO_2," *Applied Catalysis A: General,* vol. 429, pp. 31-38, 2012.

[39] A. Gasparotto, D. Barreca, D. Bekermann, A. Devi, R. A. Fischer, P. Fornasiero, *et al.*, "F-doped Co_3O_4 photocatalysts for sustainable H2 generation from water/ethanol," *Journal of the American Chemical Society,* vol. 133, pp. 19362-19365, 2011.

[40] S. Kuriakose, B. Satpati, and S. Mohapatra, "Highly efficient photocatalytic degradation of organic dyes by Cu doped ZnO nanostructures," *Physical Chemistry Chemical Physics,* vol. 17, pp. 25172-25181, 2015.

[41] M. Janczarek, A. Zielińska-Jurek, I. Markowska, and J. Hupka, "Transparent thin films of Cu–TiO_2 with visible light photocatalytic activity," *Photochemical & Photobiological Sciences,* vol. 14, pp. 591-596, 2015.

[42] E. Aazam, "Photocatalytic oxidation of methylene blue dye under visible light by Ni doped Ag_2S nanoparticles," *Journal of Industrial and Engineering Chemistry,* vol. 20, pp. 4033-4038, 2014.

[43] P. Saharan, G. R. Chaudhary, S. Lata, S. Mehta, and S. Mor, "Ultra fast and effective treatment of dyes from water with the synergistic effect of Ni doped ZnO nanoparticles and ultrasonication," *Ultrasonics sonochemistry,* vol. 22, pp. 317-325, 2015.

[44] G. Chen, X. Si, J. Yu, H. Bai, and X. Zhang, "Doping nano-Co_3O_4 surface with bigger nanosized Ag and its photocatalytic properties for visible light photodegradation of organic dyes," *Applied Surface Science,* vol. 330, pp. 191-199, 2015.

[45] A. Khanna and V. K. Shetty, "Solar light induced photocatalytic degradation of Reactive Blue 220 (RB-220) dye with highly efficient Ag@ TiO_2 core–shell nanoparticles: a comparison with UV photocatalysis," *Solar Energy,* vol. 99, pp. 67-76, 2014.

References

[46] C. Y. Ma, Z. Mu, J. J. Li, Y. G. Jin, J. Cheng and G. Q. Lu, "Mesoporous Co_3O_4 and Au/Co_3O_4 catalysts for low-temperature oxidation of trace ethylene," *Journal of the American Chemical Society,* vol. 132, pp. 2608-2613, 2010.

[47] A. Khataee, M. Hosseini, Y. Hanifehpour, M. Safarpour, and S. Joo, "Hydrothermal synthesis and characterization of Nd-doped ZnSe nanoparticles with enhanced visible light photocatalytic activity," *Research on Chemical Intermediates,* vol. 40, pp. 495-508, 2014.

[48] Y. Bessekhouad, D. Robert, and J. Weber, "Bi_2S_3/TiO_2 and CdS/TiO_2 heterojunctions as an available configuration for photocatalytic degradation of organic pollutant," *Journal of Photochemistry and Photobiology A: Chemistry,* vol. 163, pp. 569-580, 2004.

[49] C. Wang, R. L. Thompson, J. Baltrus, and C. Matranga, "Visible light photoreduction of CO_2 using $CdSe/Pt/TiO_2$ heterostructured catalysts," *The Journal of Physical Chemistry Letters,* vol. 1, pp. 48-53, 2009.

[50] C. Wang, R. L. Thompson, P. Ohodnicki, J. Baltrus, and C. Matranga, "Size-dependent photocatalytic reduction of CO_2 with PbS quantum dot sensitized TiO_2 heterostructured photocatalysts," *Journal of Materials Chemistry,* vol. 21, pp. 13452-13457, 2011.

[51] S. Cho, J.-W. Jang, J. Kim, J. S. Lee, W. Choi, and K.-H. Lee, "Three-dimensional type II ZnO/ZnSe heterostructures and their visible light photocatalytic activities," *Langmuir,* vol. 27, pp. 10243-10250, 2011.

[52] M. Long, W. Cai, J. Cai, B. Zhou, X. Chai, and Y. Wu, "Efficient photocatalytic degradation of phenol over $Co_3O_4/BiVO_4$ composite under visible light irradiation," *The Journal of Physical Chemistry B,* vol. 110, pp. 20211-20216, 2006.

[53] P. Chen, T.-Y. Xiao, H.-H. Li, J.-J. Yang, Z. Wang, H.-B. Yao, *et al.*, "Nitrogen-doped graphene/ZnSe nanocomposites: hydrothermal synthesis and their enhanced electrochemical and photocatalytic activities," *Acs Nano,* vol. 6, pp. 712-719, 2011.

[54] S. Cho, J.-W. Jang, J. S. Lee, and K.-H. Lee, "Porous ZnO–ZnSe nanocomposites for visible light photocatalysis," *Nanoscale,* vol. 4, pp. 2066-2071, 2012.

[55] M. Pudukudy and Z. Yaakob, "Sol-gel synthesis, characterisation, and photocatalytic activity of porous spinel Co_3O_4 nanosheets," *Chemical Papers,* vol. 68, pp. 1087-1096, 2014.

[56] X. Lou, J. Han, W. Chu, X. Wang, and Q. Cheng, "Synthesis and photocatalytic property of Co_3O_4 nanorods," *Materials Science and Engineering: B,* vol. 137, pp. 268-271, 2007.

[57] S. Xiong, B. Xi, C. Wang, G. Xi, X. Liu, and Y. Qian, "Solution-Phase Synthesis and High Photocatalytic Activity of Wurtzite ZnSe Ultrathin Nanobelts: A General Route to 1D Semiconductor Nanostructured Materials," *Chemistry-A European Journal,* vol. 13, pp. 7926-7932, 2007.

[58] H. Tong, S. Ouyang, Y. Bi, N. Umezawa, M. Oshikiri, and J. Ye, "Nano-photocatalytic materials: possibilities and challenges," *Advanced materials,* vol. 24, pp. 229-251, 2012.

[59] M. J. Nalbandian, M. Zhang, J. Sanchez, Y.-H. Choa, D. M. Cwiertny, and N. V. Myung, "Synthesis and optimization of $BiVO_4$ and co-catalyzed $BiVO_4$ nanofibers for visible light-activated photocatalytic degradation of aquatic micropollutants," *Journal of Molecular Catalysis A: Chemical,* vol. 404, pp. 18-26, 2015.

[60] L. F. Cueto, G. T. Martínez, G. Zavala, and E. M. Sánchez, "Surface characterization and CO_2 reduction using electrodeposited silver particles over TiO2 thin film," in *Journal of Nano Research*, 2010, pp. 89-100.

[61] C. Zhao, A. Krall, H. Zhao, Q. Zhang, and Y. Li, "Ultrasonic spray pyrolysis synthesis of Ag/TiO_2 nanocomposite photocatalysts for simultaneous H_2 production and CO_2 reduction," *international journal of hydrogen energy,* vol. 37, pp. 9967-9976, 2012.

[62] D. Sui, X. Yin, H. Dong, S. Qin, J. Chen, and W. Jiang, "Photocatalytically reducing CO_2 to methyl formate in methanol over Ag loaded $SrTiO_3$ nanocrystal catalysts," *Catalysis letters,* vol. 142, pp. 1202-1210, 2012.

[63] Y. Kohno, H. Hayashi, S. Takenaka, T. Tanaka, T. Funabiki, and S. Yoshida, "Photo-enhanced reduction of carbon dioxide with hydrogen over Rh/TiO_2," *Journal of Photochemistry and photobiology A: Chemistry,* vol. 126, pp. 117-123, 1999.

[64] H.-C. Yang, H.-Y. Lin, Y.-S. Chien, J. C.-S. Wu, and H.-H. Wu, "Mesoporous TiO2/SBA-15, and Cu/TiO_2/SBA-15 composite photocatalysts for photoreduction of CO_2 to methanol," *Catalysis Letters*, vol. 131, pp. 381-387, 2009.

[65] Q. Shen, Z. Chen, X. Huang, M. Liu, and G. Zhao, "High-yield and selective photoelectrocatalytic reduction of CO_2 to formate by metallic copper decorated Co_3O_4 nanotube arrays," *Environmental science & technology*, vol. 49, pp. 5828-5835, 2015.

[66] M. Ni, M. K. Leung, D. Y. Leung, and K. Sumathy, "A review and recent developments in photocatalytic water-splitting using TiO2 for hydrogen production," *Renewable and Sustainable Energy Reviews*, vol. 11, pp. 401-425, 2007.

[67] T. Jia, A. Kolpin, C. Ma, R. C.-T. Chan, W.-M. Kwok, and S. E. Tsang, "A graphene dispersed CdS–MoS_2 nanocrystal ensemble for cooperative photocatalytic hydrogen production from water," *Chemical Communications*, vol. 50, pp. 1185-1188, 2014.

[68] M. Z. Rahman, J. Ran, Y. Tang, M. Jaroniec, and S. Z. Qiao, "Surface activated carbon nitride nanosheets with optimized electro-optical properties for highly efficient photocatalytic hydrogen production," *Journal of Materials Chemistry A*, vol. 4, pp. 2445-2452, 2016.

[69] A. S. Adeleye, A. A. Keller, R. J. Miller, and H. S. Lenihan, "Persistence of commercial nanoscaled zero-valent iron (nZVI) and by-products," *Journal of Nanoparticle Research*, vol. 15, p. 1418, 2013.

[70] R. Köber, H. Hollert, G. Hornbruch, M. Jekel, A. Kamptner and N. Klaas, "Nanoscale zero-valent iron flakes for groundwater treatment," *Environmental earth sciences*, vol. 72, p. 1, 2014.

[71] M. Humayun, Z. Li, L. Sun, X. Zhang, F. Raziq, and A. Zada, "Coupling of nanocrystalline anatase TiO_2 to porous nanosized LaFeO3 for efficient visible-light photocatalytic degradation of pollutants," *Nanomaterials*, vol. 6, p. 22, 2016.

[72] T. S. Jamil, T. A. Gad-Allah, M. E. Ali, and M. N. Momba, "Utilization of nano size TiO_2 for degradation of phenol enrich water by solar photocatalytic oxidation," *Desalination and Water Treatment*, vol. 53, pp. 1101-1106, 2015.

[73] D. Valechha, S. Lokhande, M. Klementova, J. Subrt, S. Rayalu, and N. Labhsetwar, "Study of nano-structured ceria for catalytic CO oxidation," *Journal of Materials Chemistry,* vol. 21, pp. 3718-3725, 2011.

[74] X. Wang, J. A. Rodriguez, J. C. Hanson, D. Gamarra, A. Martínez-Arias, and M. Fernández-García, "In situ studies of the active sites for the water gas shift reaction over Cu− CeO_2 catalysts: complex interaction between metallic copper and oxygen vacancies of ceria," *The Journal of Physical Chemistry B,* vol. 110, pp. 428-434, 2006.

[75] M. Saito, M. Itoh, J. Iwamoto, C.-Y. Li, and K.-i. Machida, "Synergistic Effect of MgO and CeO_2 as a Support for Ruthenium Catalysts in Ammonia Synthesis," *Catalysis letters,* vol. 106, pp. 107-110, 2006.

[76] T. Garcia, B. Solsona, and S. H. Taylor, "Nano-crystalline ceria catalysts for the abatement of polycyclic aromatic hydrocarbons," *Catalysis Letters,* vol. 105, pp. 183-189, 2005.

[77] E. N. Ndifor, T. Garcia, B. Solsona, and S. H. Taylor, "Influence of preparation conditions of nano-crystalline ceria catalysts on the total oxidation of naphthalene, a model polycyclic aromatic hydrocarbon," *Applied Catalysis B: Environmental,* vol. 76, pp. 248-256, 2007.

[78] V. K. Gupta and T. A. Saleh, "Sorption of pollutants by porous carbon, carbon nanotubes and fullerene-An overview," *Environmental science and pollution research,* vol. 20, pp. 2828-2843, 2013.

[79] R. Q. Long and R. T. Yang, "Carbon nanotubes as superior sorbent for dioxin removal," *Journal of the American Chemical Society,* vol. 123, pp. 2058-2059, 2001.

[80] M. F. Ehsan and T. He, "In situ synthesis of ZnO/ZnTe common cation heterostructure and its visible-light photocatalytic reduction of CO_2 into CH_4," *Applied Catalysis B: Environmental,* vol. 166, pp. 345-352, 2015.

[81] M. F. Ehsan, M. N. Ashiq, and T. He, "Hollow and mesoporous ZnTe microspheres: synthesis and visible-light photocatalytic reduction of carbon dioxide into methane," *RSC Advances,* vol. 5, pp. 6186-6194, 2015.

[82] D. Wang, Z. Xu, Q. Luo, X. Li, J. An, and R. Yin, "Preparation and visible-light photocatalytic performances of g-C_3N_4 surface hybridized with a small amount of CdS nanoparticles," *Journal of materials science,* vol. 51, pp. 893-902, 2016.

References

[83] C. Han, L. Ge, C. Chen, Y. Li, X. Xiao and Y. Zhang, "Novel visible light induced Co_3O_4-g C_3N_4 heterojunction photocatalysts for efficient degradation of methyl orange," *Applied Catalysis B: Environmental,* vol. 147, pp. 546-553, 2014.

[84] A. Sadollahkhani, Z. H. Ibupoto, S. Elhag, O. Nur, and M. Willander, "Photocatalytic properties of different morphologies of CuO for the degradation of Congo red organic dye," *Ceramics International,* vol. 40, pp. 11311-11317, 2014.

[85] T. T. ThanhThuy, H. Feng, and Q. Cai, "Photocatalytic degradation of pentachlorophenol on ZnSe/TiO_2 supported by photo-Fenton system," *Chemical engineering journal,* vol. 223, pp. 379-387, 2013.

[86] M. S. Khan, M. N. Ashiq, M. F. Ehsan, T. He, and S. Ijaz, "Controlled synthesis of cobalt telluride superstructures for the visible light photo-conversion of carbon dioxide into methane," *Applied Catalysis A: General,* vol. 487, pp. 202-209, 2014.

[87] M. Ren, S. Yuan, L. Su, and Z. Zhou, "Chrysanthemum-like Co_3O_4 architectures: hydrothermal synthesis and lithium storage performances," *Solid State Sciences,* vol. 14, pp. 451-455, 2012.

[88] M. G. Pia, G. Weidenspointner, M. Augelli, L. Quintieri, P. Saracco and M. Sudhakar, "PIXE simulation with Geant4," *IEEE transactions on nuclear science,* vol. 56, pp. 3614-3649, 2009.

[89] H. Zhou, M. Kang, D. Wu, and B. Lv, "Synthesis and catalytic property of facet-controlled Co_3O_4 structures enclosed by (111) and (113) facets," *CrystEngComm,* vol. 18, pp. 5456-5462, 2016.

[90] L. Jiang and Y. J. Zhu, "A general solvothermal route to the synthesis of CoTe, Ag_2Te/Ag, and CdTe nanostructures with varied morphologies," *European Journal of Inorganic Chemistry,* vol. 2010, pp. 1238-1243, 2010.

[91] F. Gu, S. F. Wang, M. K. Lü, G. J. Zhou, D. Xu, and D. R. Yuan, "Photoluminescence properties of SnO_2 nanoparticles synthesized by sol– gel method," *The Journal of Physical Chemistry B,* vol. 108, pp. 8119-8123, 2004.

[92] F. Gu, C. Li, Y. Hu, and L. Zhang, "Synthesis and optical characterization of Co_3O_4 nanocrystals," *Journal of Crystal Growth,* vol. 304, pp. 369-373, 2007.

[93] G. Wang, X. Shen, J. Horvat, B. Wang, H. Liu and D. Wexler, "Hydrothermal synthesis and optical, magnetic, and supercapacitance properties of

nanoporous cobalt oxide nanorods," *The Journal of Physical Chemistry C,* vol. 113, pp. 4357-4361, 2009.

[94] D. Barreca, C. Massignan, S. Daolio, M. Fabrizio, C. Piccirillo and L. Armelao, "Composition and microstructure of cobalt oxide thin films obtained from a novel cobalt (II) precursor by chemical vapor deposition," *Chemistry of Materials,* vol. 13, pp. 588-593, 2001.

[95] K. J. Kim and Y. R. Park, "Optical investigation of charge-transfer transitions in spinel Co_3O_4," *Solid state communications,* vol. 127, pp. 25-28, 2003.

[96] V. Shinde, S. Mahadik, T. Gujar, and C. Lokhande, "Supercapacitive cobalt oxide (Co_3O_4) thin films by spray pyrolysis," *Applied Surface Science,* vol. 252, pp. 7487-7492, 2006.

[97] A. Louardi, A. Rmili, F. Ouachtari, A. Bouaoud, B. Elidrissi, and H. Erguig, "Characterization of cobalt oxide thin films prepared by a facile spray pyrolysis technique using perfume atomizer," *Journal of Alloys and Compounds,* vol. 509, pp. 9183-9189, 2011.

[98] R. Xu and H. C. Zeng, "Self-generation of tiered surfactant superstructures for one-pot synthesis of Co_3O_4 nanocubes and their close-and non-close-packed organizations," *Langmuir,* vol. 20, pp. 9780-9790, 2004.

[99] N. A. Barakat, M. S. Khil, F. A. Sheikh, and H. Y. Kim, "Synthesis and optical properties of two cobalt oxides (CoO and Co3O4) nanofibers produced by electrospinning process," *The Journal of Physical Chemistry C,* vol. 112, pp. 12225-12233, 2008.

[100] C. Priester, Y. Foulon, and G. Allan, "Role of localized interface states at type-II heterojunctions," *Physical Review B,* vol. 49, p. 2919, 1994.

[101] M.-J. Kim, Y. I. Choi, S. W. Joo, M. Kang, and Y. Sohn, "Synthesis of Er and Yb-doped cubic and hexagonal phase ZnSe nano-assembled microspheres and their photocatalytic activities," *Ceramics International,* vol. 40, pp. 16051-16059, 2014.

[102] L. Yang, R. Zhou, J. Lan, Q. Zhang, G. Cao, and J. Zhu, "Efficient band alignment for Zn x Cd 1− x Se QD-sensitized TiO_2 solar cells," *Journal of Materials Chemistry A,* vol. 2, pp. 3669-3676, 2014.